NASA/CR–2010-216699

Design of Structurally Efficient Tapered Struts (SETS)

Ravi Deo, Harry Benner, and Dawson Vincent
Northrop Grumman Corporation, Integrated Systems, El Segundo, California

Eric Olason
Park Aerospace Structures Corporation, Lynnwood, Washington

Richard Harrison
Northrop Grumman Corporation, Space Technology, San Bernardino, California

May 2010

NASA STI Program . . . in Profile

Since its founding, NASA has been dedicated to the advancement of aeronautics and space science. The NASA scientific and technical information (STI) program plays a key part in helping NASA maintain this important role.

The NASA STI program operates under the auspices of the Agency Chief Information Officer. It collects, organizes, provides for archiving, and disseminates NASA's STI. The NASA STI program provides access to the NASA Aeronautics and Space Database and its public interface, the NASA Technical Report Server, thus providing one of the largest collections of aeronautical and space science STI in the world. Results are published in both non-NASA channels and by NASA in the NASA STI Report Series, which includes the following report types:

- TECHNICAL PUBLICATION. Reports of completed research or a major significant phase of research that present the results of NASA programs and include extensive data or theoretical analysis. Includes compilations of significant scientific and technical data and information deemed to be of continuing reference value. NASA counterpart of peer-reviewed formal professional papers, but having less stringent limitations on manuscript length and extent of graphic presentations.

- TECHNICAL MEMORANDUM. Scientific and technical findings that are preliminary or of specialized interest, e.g., quick release reports, working papers, and bibliographies that contain minimal annotation. Does not contain extensive analysis.

- CONTRACTOR REPORT. Scientific and technical findings by NASA-sponsored contractors and grantees.

- CONFERENCE PUBLICATION. Collected papers from scientific and technical conferences, symposia, seminars, or other meetings sponsored or co-sponsored by NASA.

- SPECIAL PUBLICATION. Scientific, technical, or historical information from NASA programs, projects, and missions, often concerned with subjects having substantial public interest.

- TECHNICAL TRANSLATION. English-language translations of foreign scientific and technical material pertinent to NASA's mission.

Specialized services also include creating custom thesauri, building customized databases, and organizing and publishing research results.

For more information about the NASA STI program, see the following:

- Access the NASA STI program home page at *http://www.sti.nasa.gov*

- E-mail your question via the Internet to help@sti.nasa.gov

- Fax your question to the NASA STI Help Desk at 443-757-5803

- Phone the NASA STI Help Desk at 443-757-5802

- Write to:
  NASA STI Help Desk
  NASA Center for AeroSpace Information
  7115 Standard Drive
  Hanover, MD 21076-1320

NASA/CR–2010-216699

Design of Structurally Efficient Tapered Struts (SETS)

Ravi Deo, Harry Benner, and Dawson Vincent
Northrop Grumman Corporation, Integrated Systems, El Segundo, California

Eric Olason
Park Aerospace Structures Corporation, Lynnwood, Washington

Richard Harrison
Northrop Grumman Corporation, Space Technology, San Bernardino, California

National Aeronautics and
Space Administration

Langley Research Center
Hampton, Virginia 23681-2199

Prepared for Langley Research Center
under Contract NNL04AA13B

May 2010

Available from:

NASA Center for AeroSpace Information
7115 Standard Drive
Hanover, MD 21076-1320
443-757-5802

CONTENTS

APPENDICES

ILLUSTRATIONS

FOREWORD

This report documents work completed on Design and Manufacture of Structurally Efficient Tapered Struts (abbreviated SETS), a task order under National Aeronautics and Space Administration (NASA) Contract NNL04AA13B. The work was performed by Northrop Grumman's Integrated Systems, Western Region, El Segundo, California. Dawn Jegley, NASA Langley Research Center, was the NASA contracting officer's technical representative. Ravi Deo was program manager for the Northrop Grumman Corporation. Harry Benner performed the closed-form analyses and the sensitivity studies to arrive at optimum designs; Richard Harrison developed the ABAQUS models and conducted analysis of design details; Dawson Vincent was Northrop Grumman Corporation's manufacturing liaison with Park Aerospace Corporation, the manufacturer of the demonstration strut; and Eric Olason was Park Aerospace Corporation's program manager responsible for designing and fabricating the demonstration strut. Greg Strand of Park Aerospace Corporation provided technical guidance to the team.

SUMMARY

A study was conducted to develop mass efficient composite struts for use in truss structures envisioned for spacecraft components such as the lunar lander airframe. This analytical methodology development and a manufacturing demonstration article fabrication study resulted in a 10-foot-long, 6-inch-diameter IM7/8552 strut designed to carry 110 kips in axial compression. Park Aerospace Corporation of Lynwood, Washington, fabricated the strut.

A closed-form design methodology for composite struts was developed using well established analyses to predict Euler buckling, local wall buckling, compression strength, damage tolerance, and interlaminar shear at geometric gradients. The methodology was coded in a spreadsheet suitable for convenient and rapid sizing of tapered composite struts. This spreadsheet analysis was used to determine the influence of several variables such as material stiffness, strut diameter, and material allowables on strut weight for given loading conditions. Results showed that a 110 kip load capacity strut would weigh the least if it were fabricated using IM7/8552 and with a diameter of 7 inches. However, for a 44 kip strut, the lowest weight was realized using M55J/8552, also with a cylinder diameter of 7 inches. This design and analysis methodology was compared and contrasted with Park Aerospace's semiempirical design methodology. The comparison showed that, while the Park Aerospace design method was well suited to preliminary sizing for a conservative design, the closed-form-analyses-based spreadsheet accounts for all possible failure modes and is a good optimum strut design tool. An ABAQUS model of the strut was also developed to understand local phenomena such as at the load transfer mechanisms in the embedded ferrule to composite interfaces.

The manufacturing demonstration article was fabricated to validate the process and to understand the dependence of buckling critical strut geometry imperfections on the tooling and processes used. The Park Aerospace patented process is described in the report and produced a 127-inch strut with less than 0.08 percent initial bow. The completed strut weighed 26.28 pounds as compared to the predicted weight of 28.28 pounds.

The report concludes with a set of recommendations for future work in analytical design and analysis methodology enhancements and for strut manufacturing process improvements.

INTRODUCTION

Purpose and Objectives

The purpose of the study reported here was to develop composite tapered struts for use in structurally efficient truss structures. These truss structures promise weight savings payoffs in spacecraft components such as the lunar lander airframe (Figure 1), components for use on the lunar surface, aircraft, and spacecraft deployable structures. Mass savings in the upper stages are especially desirable because the lunar lander mass multiplier for each mass unit saved can be as high as 16.

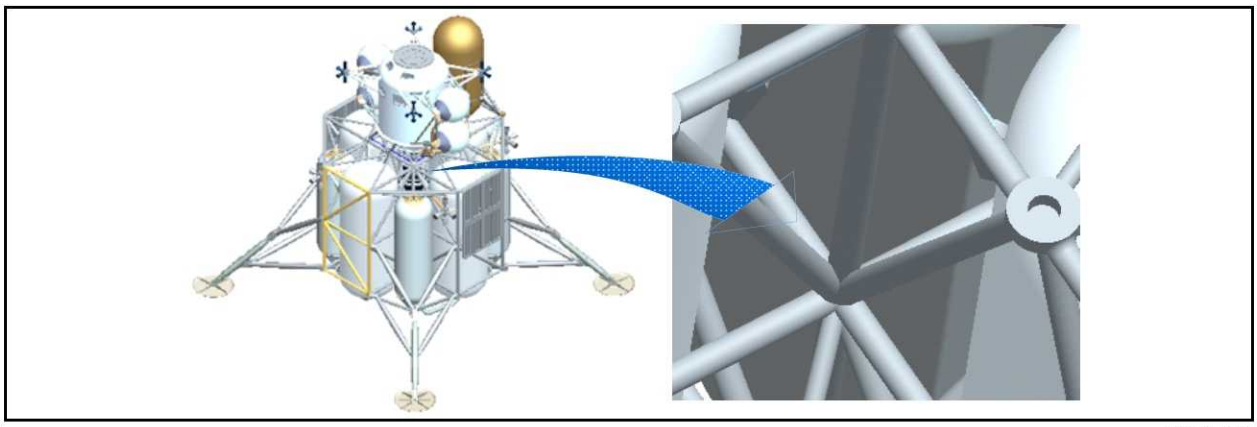

8NP79-004

Figure 1. Altair Structural Arrangement and Truss Structure Schematic

The specific objectives of the study were to: (1) conduct an analytical study resulting in a structurally efficient design of composite (e.g., carbon-epoxy) struts with the geometries and loading conditions described in Figure 2; (2) develop one or more concepts for joining the optimized strut to other structural components; and (3) build and deliver a manufacturing demonstration article large enough to show key features of the manufacturing method.

Strut ID	Length (in)	Axial Compression Load (lb)	Boundary Conditions
1	135	44,000	Pinned on Both Ends
2	127	110,000	Pinned on Both Ends

Figure 2. Geometries and Loading Conditions for Analytical Study

Technical Task Plan

The technical approach consisted of first conducting an analytical study to optimize the design of the two struts subject to the loading conditions of Figure 2. As a part of this task, a structural arrangement and concept for joining the optimized strut to other truss components was developed recognizing that, for some applications, up to eleven struts could be joined at one location at various angles. In the next subtask, a manufacturing demonstration article was built and delivered to National Aeronautics and Space Administration (NASA) Langley Research Center (LaRC). The manufacturing demonstration article was fabricated to validate the process and to understand the dependence of buckling critical strut geometry imperfections on the tooling and processes used. The analysis and design methodology developed, the optimum designs for the two struts in Figure 2, and a description of the manufacturing method used to fabricate the 127-inch demonstration article are documented in this final report.

STRUT ANALYSIS AND DESIGN

Overview

Three discrete analysis activities were performed in the development of the optimum strut design. Each has its own strengths and provides unique pieces of information leading to an improved understanding of tapered composite strut design.

The first analysis effort involved performance of a series of sensitivity studies that examined variations in material properties (e.g., fiber used), constant cross-section diameter, ply orientation distribution, size of initial imperfections, and damage-tolerance considerations. The analysis was done using an Excel sizing spreadsheet developed for this purpose. The details of this spreadsheet are provided in Appendix A.

The second analysis effort performed the detailed sizing of the manufactured 110K strut using a legacy spreadsheet that the strut manufacturer, Park Aerospace Structures Corporation, regularly employs. This spreadsheet incorporates sizing approaches and guidelines developed over years of designing and manufacturing composite struts of this type. Its specifics are outlined in Appendix B.

The final analyses effort conducted was to develop detailed ABAQUS models of the end-fitting joint and the overall strut itself. This provided a more detailed look into some of the key behaviors and capabilities of the as built 110K strut. A summary of the ABAQUS analysis results is presented in this section of the report.

Material Allowables Development

Three materials were selected for examination in the aforementioned sensitivity studies. All were tape product forms that contained graphite fibers impregnated in epoxy resin. It was assumed that fiber properties dominate the laminate behavior and that variations in resin would not produce appreciable changes in the sensitivity study results. The three fibers selected for examination were AS4, IM7, and M55J. In order to make “apples to apples” comparison studies, material properties (stiffness and allowables properties and how they vary with lay-up) were required for all three. The available, nonproprietary materials data varied widely among the three fiber types with M55J data being particularly sparse. The allowables for AS4 and M55J were “derived” from the vendor-supplied and other similar fiber data.

The fundamental approach adopted for material properties development was to first gather as much data as possible on each of the three candidate fibers from a variety of sources. Then the best database, as determined from the credibility of the source, was selected as the “baseline.” The G40-800/977-2 database adapted by NASA to IM7/977-2 was determined to be the “best” available and was used as the baseline. The databases for the other two candidate fibers were derived from this more comprehensive “baseline” database. This database has all the required material stiffness data, 1/4-inch open-hole tension and compression strain allowables as a function of the percentage of 45-degree plies, interlaminar stress allowables, and temperature knockdowns. The available AS4 and M55J lacked much of this information, most notably the variation of strain allowables with lay-up and the knockdowns associated with the 1/4-inch holes (i.e., “damaged” allowables).

AS4 and M55J databases, comparable in detail to the IM7 one, were derived by comparing key parameters available for all three fibers and factoring the IM7 database by the ratio of

selected key parameters. Which ratios to use and how to apply them were based on an understanding of material behavior and engineering judgment.

One cautionary note: no test data were available for open-hole allowables with 45-degree plies less than 25 percent. The shape of the allowables curves appear fairly flat around 25 percent 45-degree plies, indicating that the strain allowables do not decrease much below the levels at 25 percent. In fact, the curve fit equations indicate that the allowables actually begin to increase again as you approach 0 percent 45-degree plies. Physically this does not make sense and is not consistent with similar data seen on other programs. For this effort, strain allowables for <25 percent 45s were obtained by extrapolating back from the 25 percent (or 30 percent for tension) value using the slope of the curve fit equation at 25 percent 45-degree plies. In this manner the allowable strains continue to decrease with the decreasing percentage of 45s. If in reality this dropoff is more dramatic than assumed here, potentially unconservative results would be obtained when the 45-degree plies are less than 25 percent.

Sizing Sensitivity Studies

The preliminary sizing spreadsheet described in Appendix A was used to perform a variety of sizing sensitivity studies presented in this section. The intent of these studies was to provide a better understanding of how key strut design parameters influence the resulting strut weight and to identify the optimum design for both struts under consideration. Identification of the optimum features for point sizing of the two struts to the requirements of Figure 2 was obtained as a result of these sensitivity studies.

Before presenting the results, it is important to document and discuss several of the key assumptions that went into this effort. First, all sizing was done using 113°F material allowable and using end fittings that had three valleys, i.e., six ramps as shown in Figure A-1 in Appendix A. These fittings were sized outside of this spreadsheet and their geometry and weight were used as inputs in the calculations described. As such the end-fitting weight does not vary with strut design. Since these fittings are a small percentage of the overall weight of the large struts, this analytical fixity has little impact on the weight sensitivity results. Additionally, the percentages of axial load transferred at each effective ramp were set at 67 percent for the first ramp, 27 percent for the second ramp, and 6 percent for the third ramp and held constant throughout the variation in sizing. This distribution was arrived at by examining the results of the ABAQUS model. Holding these end-fitting parameters constant has negligible effect on the overall results because the fitting and end overwrap ply weights are only a small fraction of the total weight for struts of the size examined here.

Regarding the laminate itself, only the 0, +45, -45, and 90 families of laminates were considered, and no minimum gauge thickness constraints were set. Consequently, it is possible that some of these solutions, particularly the M55J ones at the larger diameters, are lighter than practically manufacturable. The user also needs to keep in mind that the key result is a theoretical thickness for the input ply orientation distribution, which does not take into account the discrete increments in laminate thickness associated with adding finite thickness lamina nor is constrained to any rules of lamination (i.e., balanced and symmetric, etc.). As such, the actual "optimum" thickness and weight, i.e., with all real-world considerations imposed, will be slightly more than the theoretical results developed here. These slight differences do not influence the trends uncovered in the SETS studies.

The following paragraphs present selected results from the sensitivity studies performed on the 110 kip strut configuration. The results are presented in terms of the overall strut weight as a function of midspan inner mold line (IML) diameter (i.e., outer diameter of the manufacturing mandrel) as a series of curves, each representing a different value of the parameter being varied.

The first sensitivity to be investigated was the influence of the initial offset assumption for an IM7 85/00/15 (85 percent 0s/0 percent 45s/15 percent 90s) laminate. The results are shown in Figure 3, which shows that variation in initial imperfection does have an appreciable impact on the resulting weight of as much as 25 to 30 percent at the 6-inch-diameter IML. Consequently, it is important to control this offset during manufacturing and select a realistic, but not overly conservative, value for use in sizing. Examination of similar struts built for an ongoing NASA contract entitled Max Launch Abort System (MLAS) [1], indicates that an initial offset value of 0.20 inch is reasonably conservative and has been used in all subsequent sizing sensitivity studies.

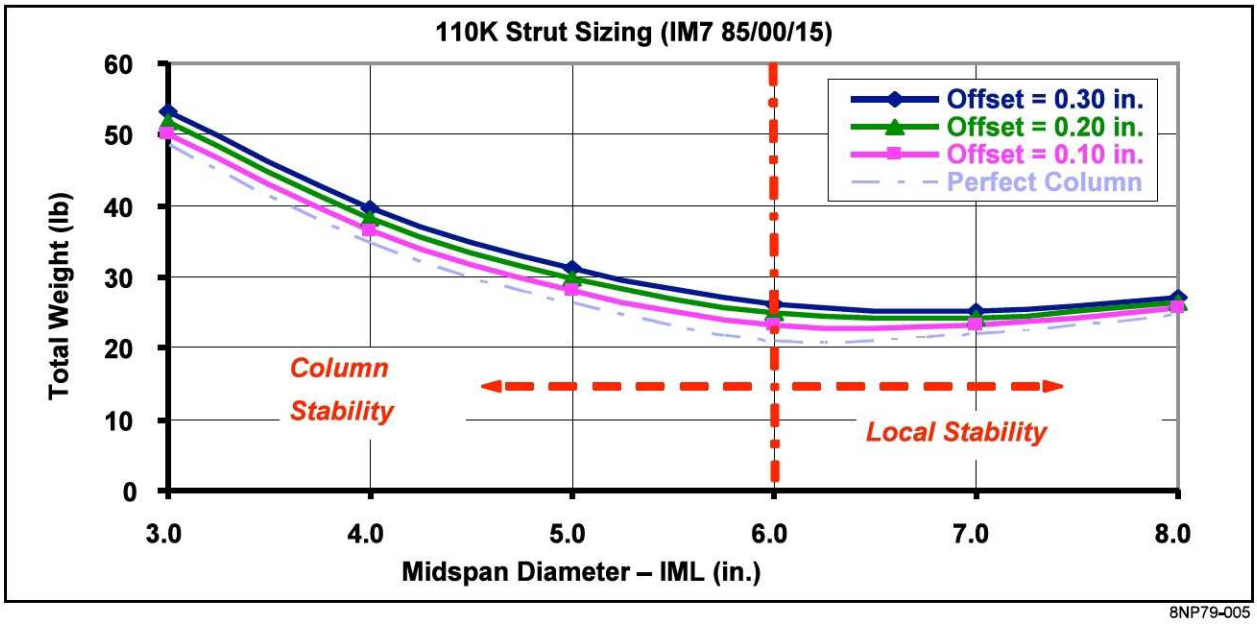

Figure 3. Influence of Initial Offset (Midspan Offset) on Strut Weight

Another interesting trend seen in these results is that the weight decreases rapidly with increasing diameter until approximately 6 inches, beyond which the weight begins to increase but at a slower rate. This occurs because the critical failure mode begins to switch from Euler-column-stability-driven strength failure modes to local cylinder instability modes. This occurs because the reduced wall thicknesses at larger diameters that are adequate for the bending stiffness (EI) needed to preclude Euler column instability are no longer adequate to preclude local buckling, and as a consequence, more wall thickness must be added back in.

The next sensitivity investigated was the influence of lay-up. For the IM7 fiber with a fixed 0.20-inch initial offset, the curves shown in Figure 4 were obtained.

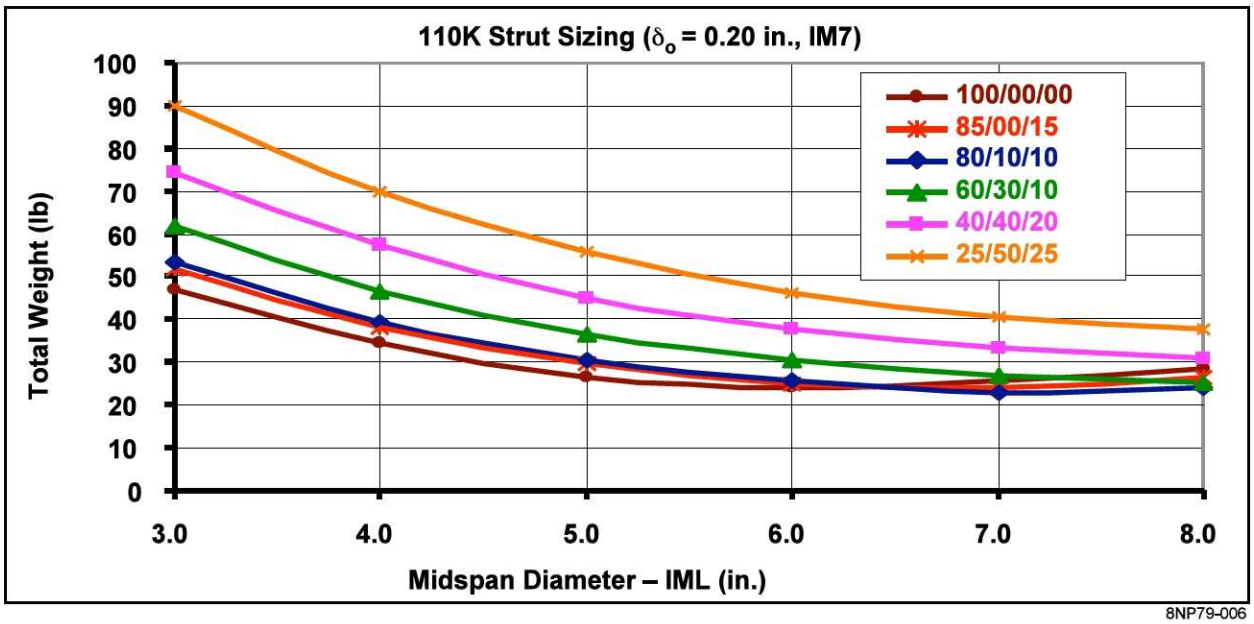

Figure 4. Influence of Lay-Up on Strut Weight

Figure 4 shows the optimum to occur at a diameter between 6 and 7 inches with the "harder" (high percent of 0s) laminates leading to lighter overall weights. The 100 percent 0-degree lay-up produces the lightest weight over the lower range of diameters because it provides the greatest EI to resist Euler buckling. However, as the diameter increases above approximately 6 inches, the local buckling mode begins to dominate, and the column begins to benefit from the addition of 45s and 90s. Increasing the combined 45-degree and 90-degree ply percentages over 25 percent clearly drives the weight up, indicating that only a relatively small percentage of these are required. Figure 4 also shows that several of the "hard" laminates produce very similar optimum weights. These trends can more clearly be seen in the comparison plots of Figures 5 and 6 in which the weights corresponding to each failure mode are plotted as a function of the diameter.

As seen in Figures 5 and 6, there is a transition between Euler-driven strength sizing below 6 inches diameter to local buckling critical sizing with the 100/0/0 laminate whereas the 60/30/10 laminate remains Euler critical over the full range of diameters examined. This implies that the softer 60/30/10 laminate has more off-axis fibers than really needed to preclude local instability and is subject to a weight penalty for it.

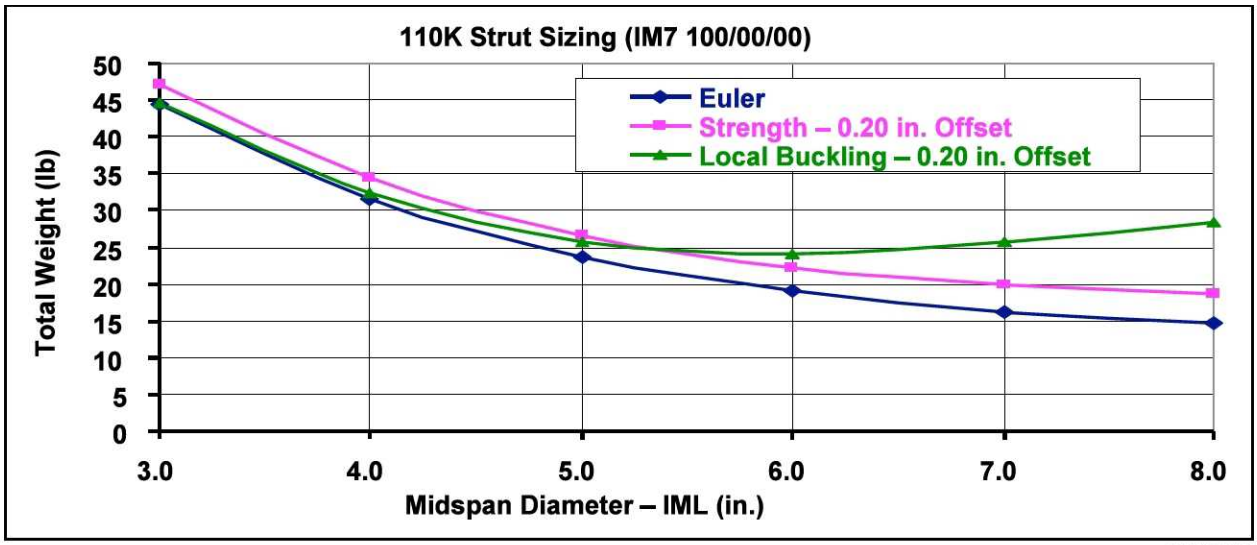

Figure 5. Strut Design Drivers as a Function of Strut Diameter for an All 0-Degree Laminate

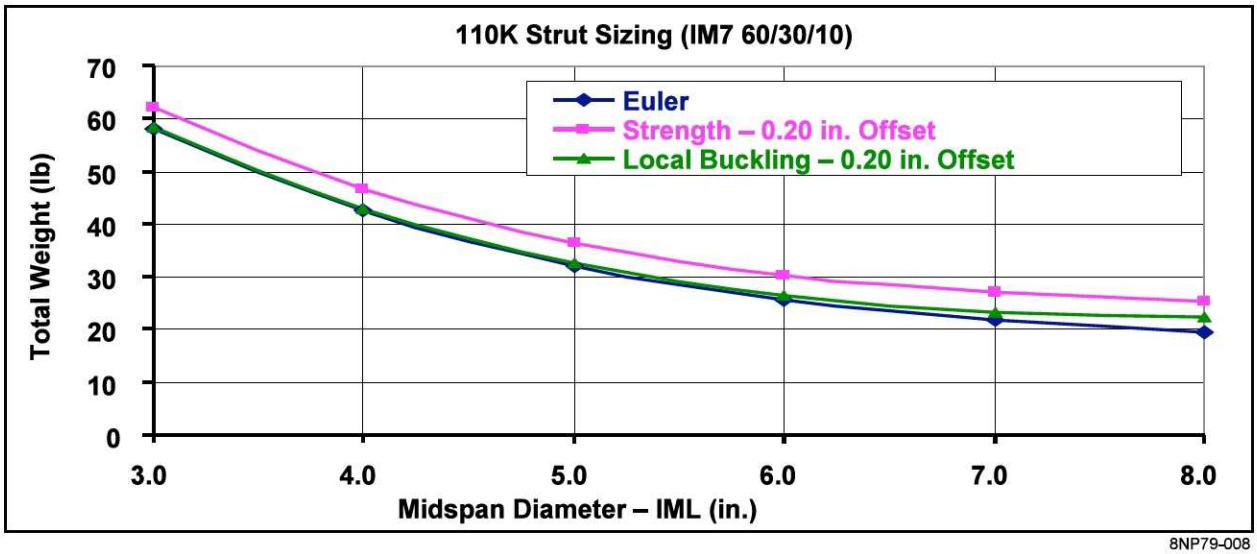

Figure 6. Strut Design Drivers as a Function of Strut Diameter for a 60/30/10 Laminate

Figure 7 compares the three candidate fibers by examining an 85/00/15 laminate with a 0.20-inch initial offset over a range of IML diameters.

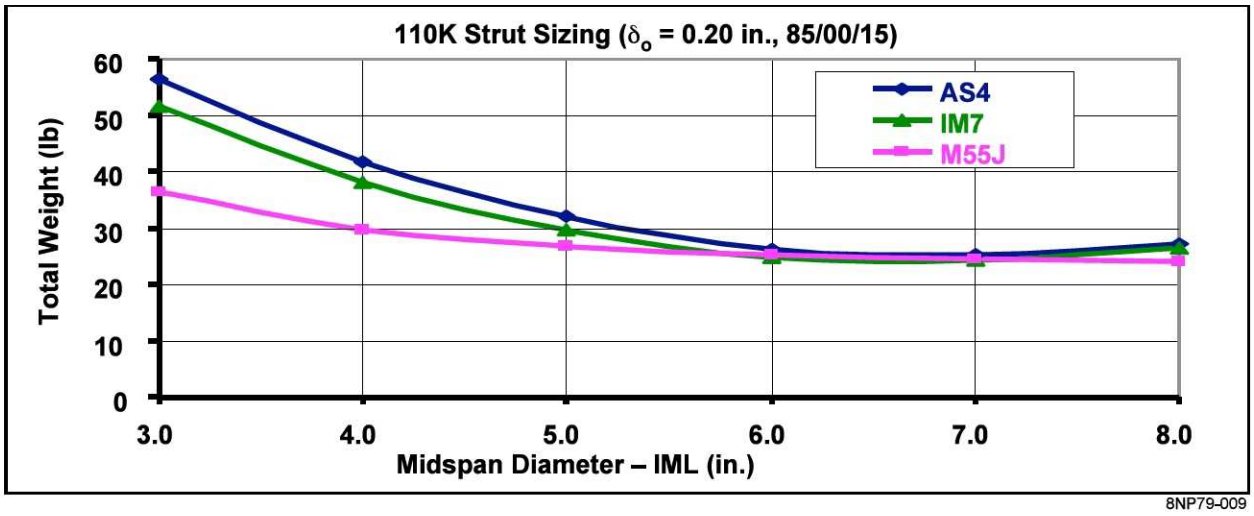

Figure 7. Influence of Fiber Type on 110 kip Strut Weight

Figure 7 clearly shows the benefit of a higher modulus at small diameters where Euler buckling dominates. The higher stiffness of the M55J fiber is not beneficial in the neighborhood of the minimum-weight diameter of 6 inches. This is due to the fact that the dominant failure mode shifts from Euler-driven strength sizing to being driven by local buckling. The M55J curve does indicate a slight benefit in the range of diameters greater than 7 inches, but this benefit may well be unrealizable after some realistic minimum gage requirements are imposed.

Figure 7 reaffirms that the optimum weight diameter for the 127-inch-long 110 kip capable strut is in the 6- to 7-inch-diameter range with little change in weight over that span. Interestingly, it also indicates that there is *no* benefit gained by using M55J (provided that no constraints on diameter exist for the particular application intended) and only a very slight weight penalty if the cheaper AS4 fiber were used.

The preceding studies have implied that stability, both local and Euler column, were the overriding design drivers and that the strength of the material might not be a major player. Figures 8 and 9, for IM7 and for M55J, respectively, examined this hypothesis by sizing using the "pristine" (i.e., undamaged) allowables instead of the open-hole (i.e., damaged or damage tolerance) allowables. A comparison of Figures 8 and 9 shows that, for an 85/00/15 laminate with a 0.20-inch offset, there is *no* benefit of using the IM7 fiber in the optimum 6- to 7-inch-diameter range, but a significant amount of benefit is realized with the M55J fiber across the entire range of diameters. This is explained by noting that the IM7 optimum sizing is driven by local buckling, which is not related to the material's strain allowable.

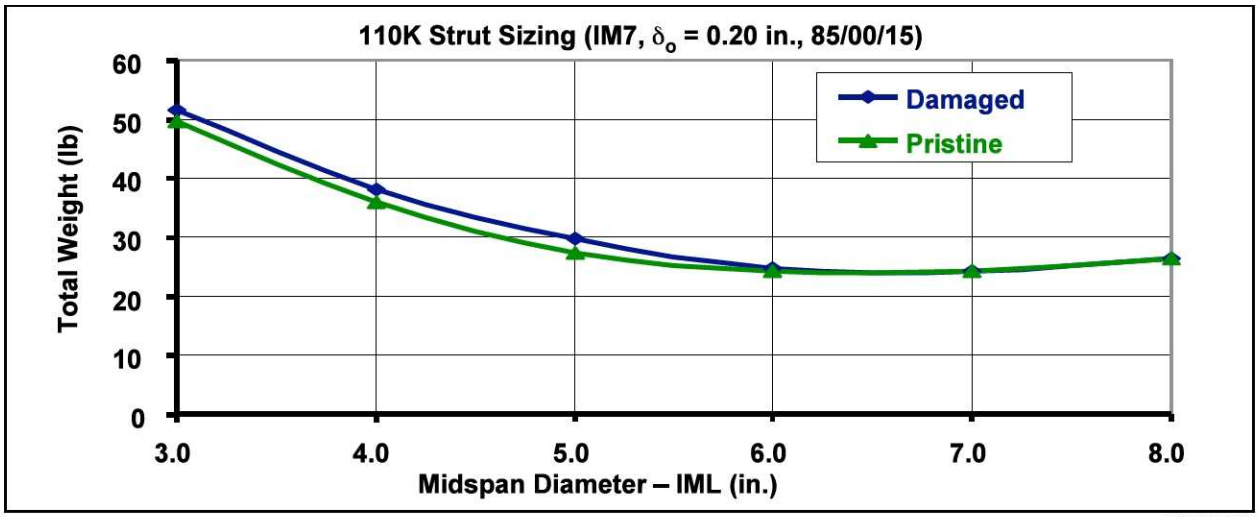

Figure 8. Strut Weight as a Function of Using Damage-Tolerance or Pristine (Undamaged) Allowables for IM7 Fiber Composites

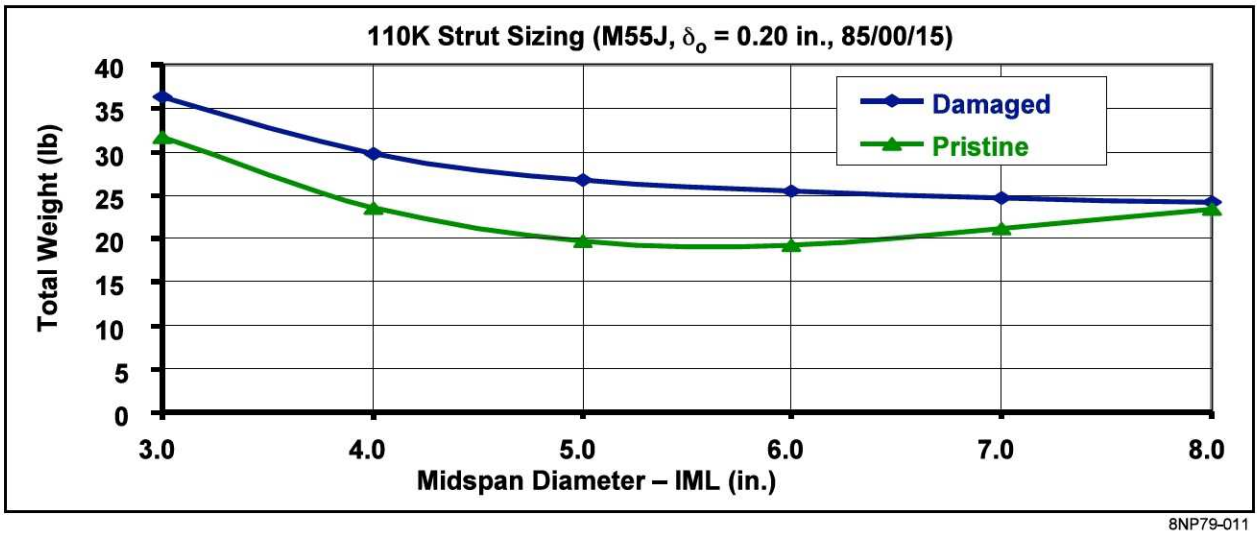

Figure 9. Strut Weight as a Function of Using Damage-Tolerance or Pristine (Undamaged) Allowables for M55J Fiber Composites

When damage tolerance is accounted for by using open-hole strain allowables, as seen in Figure 10, the M55J strut sizing and therefore weight is driven by the material strength and much less by stability. Consequently, any improvements made in the strength allowable (such as relaxing the damage-tolerance requirements) would result in lighter weight M55J struts.

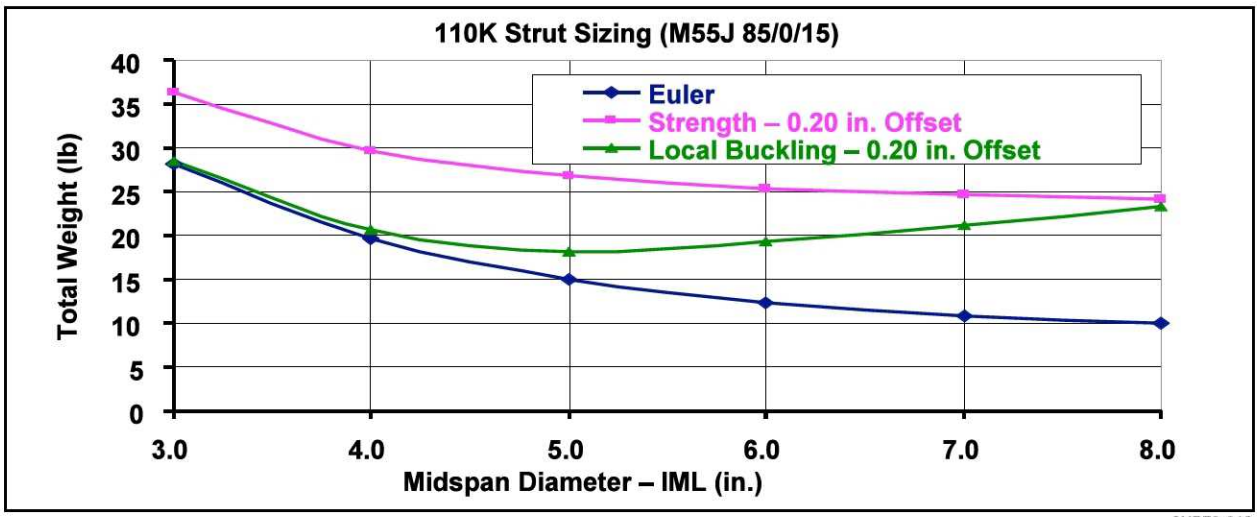

Figure 10. Strength Considerations Drive the Weight of the M55J Fiber Struts

Another interesting comparison (Figure 11) is between the IM7 fiber strut weight designed to a 1/4-inch open-hole allowable and the M55J strut weight designed to "pristine" or undamaged allowable.

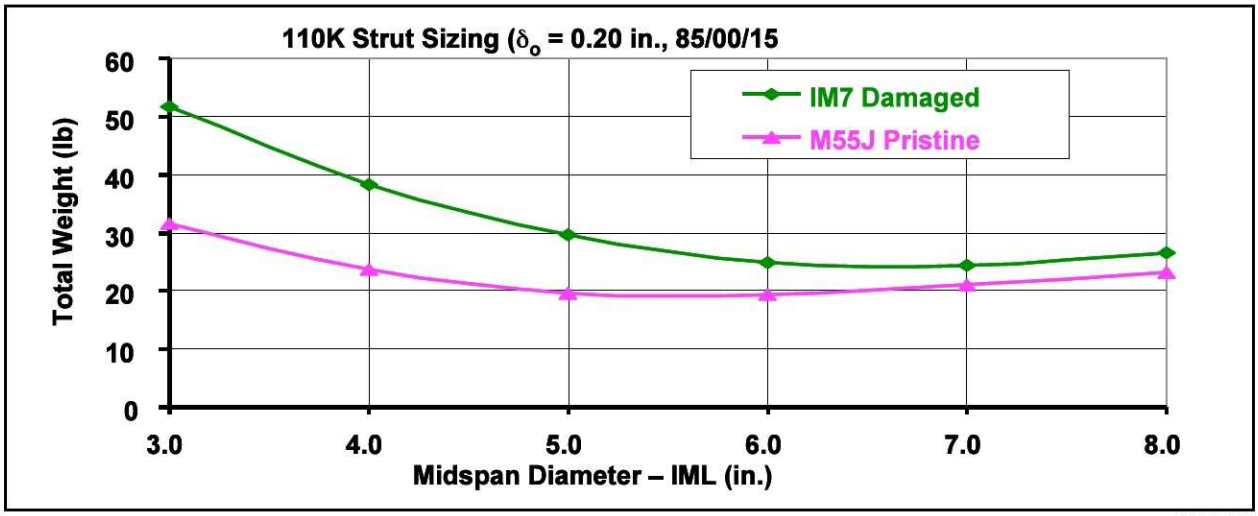

Figure 11. Influence of Fiber Type on Strut Weight if Damage-Tolerance Requirement Is Relaxed for M55J Fiber Strut

As seen in Figure 11, a reduction in weight would result for the M55J strut if the damage tolerance considerations were relaxed, more so at the lower diameters but still significant at the optimum, approximately 6 inches in diameter.

A review of the preceding sensitivity studies indicates that, for the 127-inch-long, 110 kip capable strut, the following conclusions can be drawn:

- The optimum diameter is in the 6- to 7-inch range with little variation in weight at either end of this range.

- At approximately 6 inches in diameter, the critical failure mode transitions from Euler-column-driven strength to local buckling.
- "Hard" laminate (*near*, but *not* at, 100 percent 0s) produce the lightest weights.
- Small percentages of 45s and 90s benefit the local buckling failure mode and produce lighter optimum weights than the 100 percent 0-degree laminate. However, too many of these (less than 80 percent 0-degree plies) result in a weight increase.
- There is no benefit of using M55J when a 1/4-inch open-hole allowable damage-tolerance criterion is imposed. An appreciable (>30 percent) weight savings can be obtained using M55J if damage-tolerance is not considered. Obviously an intermediate level of weight savings may be realized if a less stringent damage-tolerance criteria is imposed.
- These conclusions would change if some physical constraint prevented the strut from attaining its preferred 6-inch diameter.

The previous analyses examined the sensitivities of the 110 kip strut configuration. All of these studies were repeated for the 44 kip strut. For the most part, the resulting trends were very similar to those seen for the 110 kip strut. A good example of this can be seen in the lay-up sensitivity curves plotted in Figure 12.

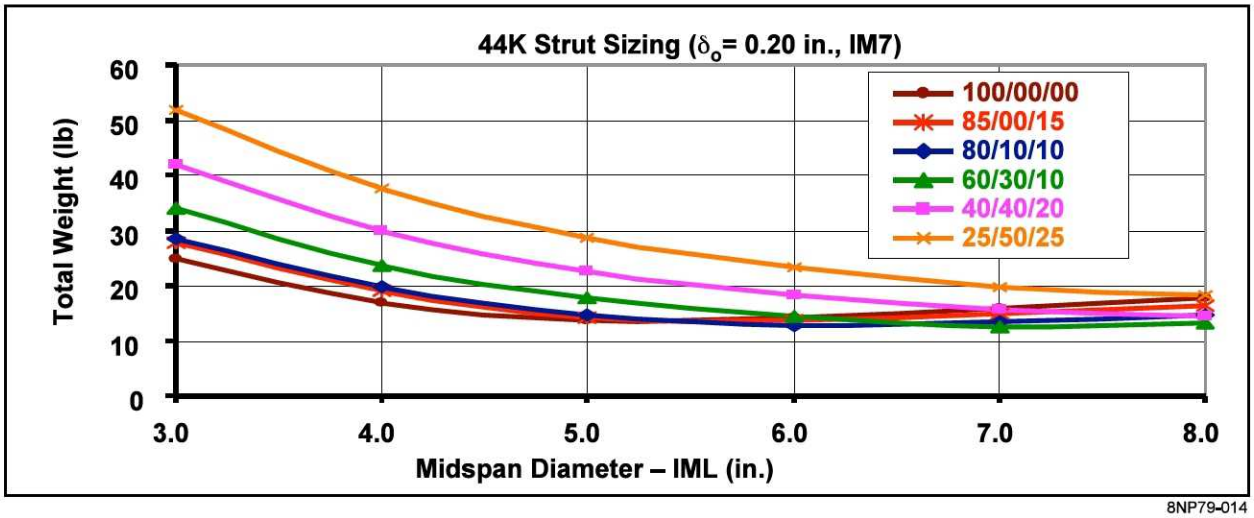

Figure 12. Weight Sensitivity to Lay-Up for 44 kip Strut With IM7 Fiber

Figure 12 shows that, as with the 110K strut, the optimum weight results from a diameter in the 6- to 7-inch range and a relatively hard lay-up. One significant difference seen in the sensitivities for the 44 kip strut is illustrated in Figure 13 where the strut weight benefits from the use of M55J fibers even with the 1/4-inch open-hole (damage-tolerance) allowable sizing criteria imposed. This occurs because the slightly longer (135 inches versus 127 inches for the 110 kip strut), lightly loaded strut is more Euler column stability driven and therefore benefits from the increased stiffness of the higher-modulus M55J fiber. Repeating the laminate lay-up sensitivity study with the more beneficial M55J fiber for the 44 kip struts results is shown in the curves in Figure 14. The optimum diameter for the 135-inch-long, 44 kip capable M55J fiber strut has now shifted to the left as compared to the 110 kip strut and is in the range of 5 to 7 inches.

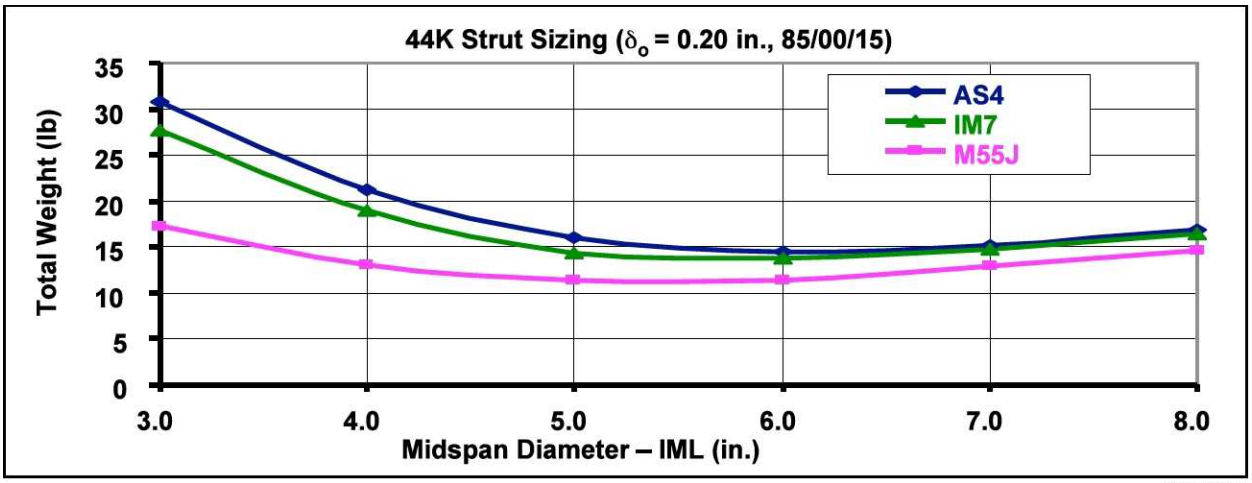

Figure 13. Influence of Fiber Type on Weight of 44 kip Strut

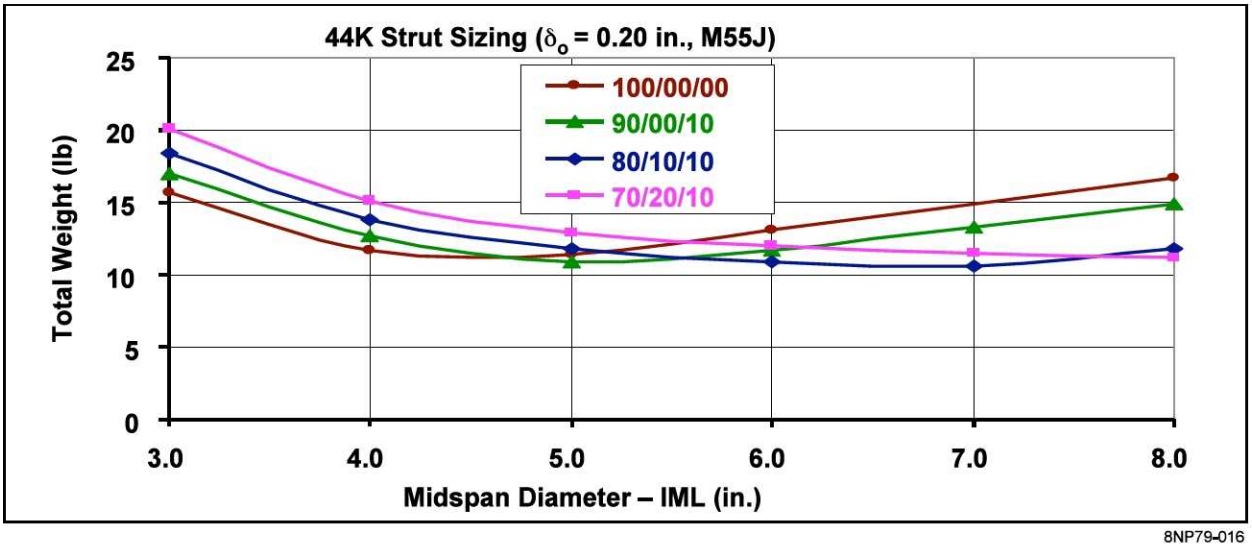

Figure 14. Weight Sensitivity to Lay-Up for 44 kip Strut With M55J Fiber

As is to be expected if damage-tolerance considerations are relaxed, the benefit of using M55J increases (Figure 15). Examining the results of the 44 kip strut sensitivity studies leads to many conclusions similar to the 110 kip strut. However, there are some significant differences that are noteworthy. Specifically:

- The optimum diameter is in the 5- to 7-inch range with little variation in weight at either end of this range.
- There *is* an appreciable benefit in using M55J (>20 percent weight savings compared to IM7) even when 1/4-inch open-hole allowable damage-tolerance criteria are imposed. This benefit is even larger if the damage-tolerance criteria are relaxed.

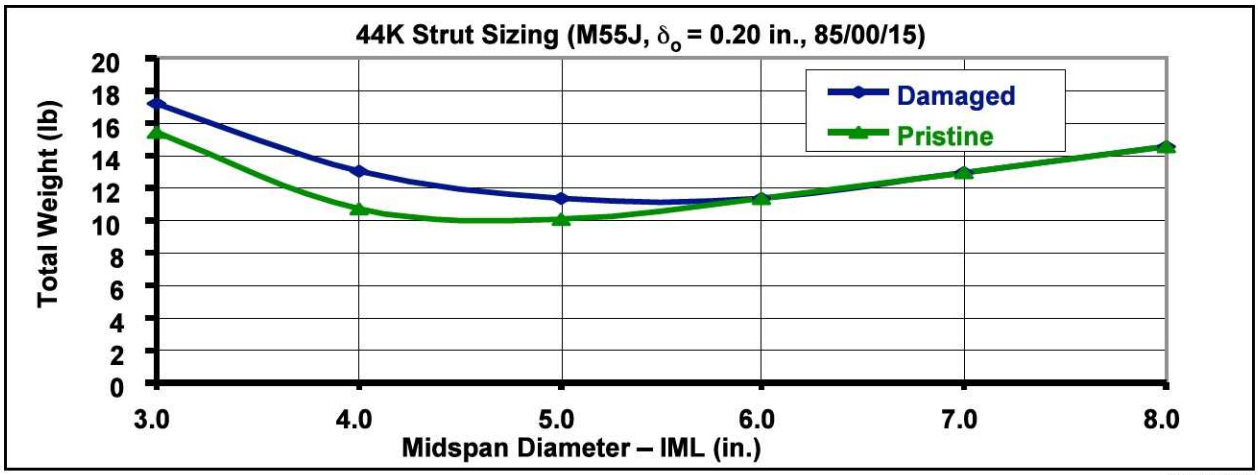

Figure 15. Benefit of Using M55J Fiber Laminates Without Imposing Damage-Tolerance Requirements

Optimum Strut Design

Based on the preceding analyses and sensitivity studies, the optimum design geometry, lay-up and material types for the 44 kip and the 110 kip strut are as shown in Figure 16. The predicted weight for the 110 kip optimum design strut is 23.37 pounds as opposed to the measured weight of 26.28 pounds for the 127-inch-long, 110 kip manufacturing demonstrator fabricated during the course of this study. These design calculations assume that the 1/4-inch open-hole sizing produces a reasonable level of damage tolerance and that the strut is built such that its midspan initial imperfection is at most 0.20 inch.

Parameter	Strut ID	
	44K	110K
Fiber	M55J	IM7
Constant Cylinder IML Diameter (in.)	7.0	7.0
Laminate (%0-degree/%+-45-degree/%90-degree	(80/10/10)	(80/10/10)
Constant Cylinder Thickness (in.)	0.0510	0.1157
End Overwrap (90-degree) Thickness (in.)	0.0973	0.1480
Weight (lb)		
Basic Strut	9.15	19.05
Overwrap Plies	0.34	0.96
End Fittings	1.10	3.36
Total	**10.59**	**23.37**

Figure 16. Optimum Design for the Two Strut Requirements of Figure 2

In conclusion, the spreadsheet sizing tool developed here enabled the rapid generation of multiple configurations required to perform sensitivity studies. It was applied to generate sensitivity curves for both the 110 kip and 44 kip strut configurations under consideration. These studies identified the key sizing drivers as well as where the optimum weight points lie. Interestingly, these studies indicated that the critical sizing and, more importantly, the critical material selection are configuration dependent. Consequently, the preferred material selection for

one strut in a cluster of many may be different than for its neighbor. Additionally, some configurations are more sensitive than others to the damage-tolerance criteria selected. Therefore, it is strongly recommended that rational, but not overly conservative, damage-tolerance criteria be developed for sizing struts of this type for Project Constellation and lunar lander applications.

Structural Arrangements

To develop a design for the end attachment fittings so that these struts can be used in a load-bearing truss, the example truss geometry shown in Figure 17 was used for visualization purposes only. The truss shown in Figure 17 was a configuration proposed for the Crew Exploration Vehicle. A schematic of a complex joint in such a truss is also shown as an inset in Figure 17.

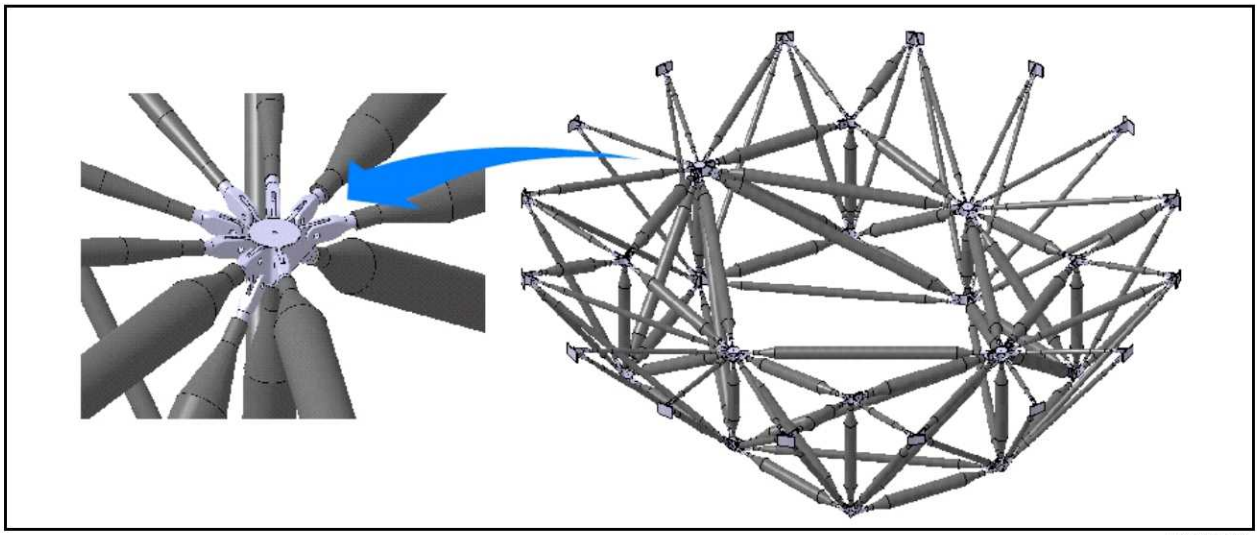

Figure 17. Example of Truss Geometry Considered for the Northrop Grumman Crew Exploration Vehicle (Inset: Joining Concept to Accommodate Multiple Struts)

In the present studies, in the absence of any member loads or directions, the generic configuration showing the relative sizes of the end-fitting in Figure 18 was developed.

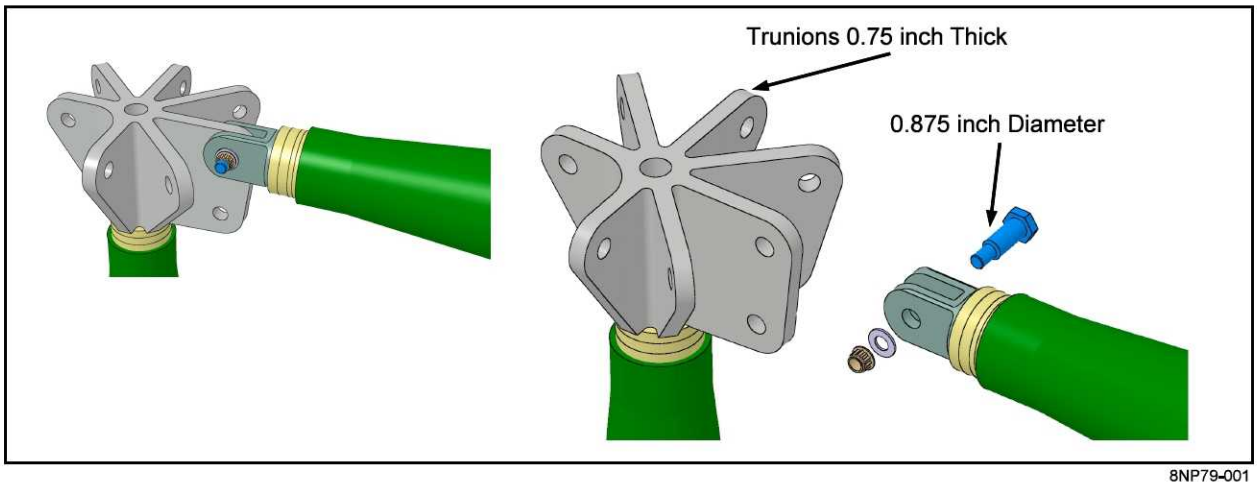

Figure 18. Clevis- and Trunnion-Ended Strut Fittings for Assembly

Details of the trunnion-ended strut and the clevis-ended strut are shown in Figures 19 and 20, respectively.

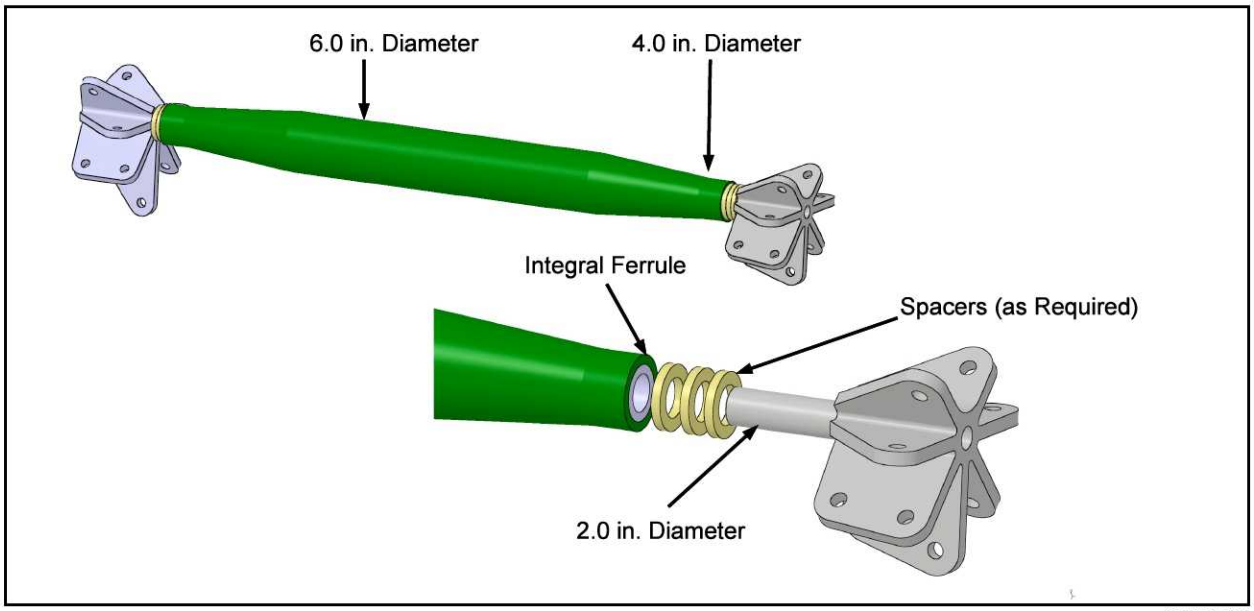

Figure 19. Trunnion End-Fitting Strut Configuration

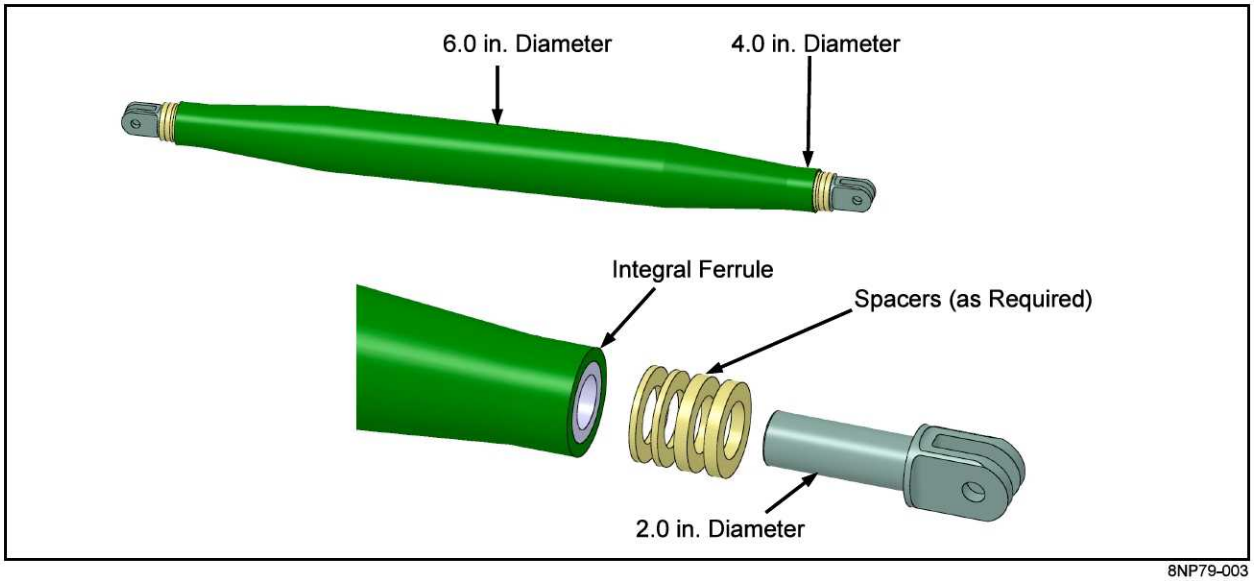

Figure 20. Clevis End-Fitting Strut Configuration

Park Aerospace Design Methodology for 110 kip Strut

The second analytical effort performed was to use Park Aerospace Structures Corporation's legacy sizing spreadsheet, described in Appendix B, to analyze the "as built" 110 kip configuration strut. This spreadsheet is similar to that used for the sensitivity studies in that it too makes margin checks for Euler column buckling, local cylinder buckling, midspan strength, interlaminar shear stress at the taper to straight section kick, and strain in the overwrap plies at the end. In addition, it makes a check on the gross interlaminar shear stress that develops along the length of the interface between the metallic fitting and the composite strut.

While not as versatile as the spreadsheet developed in Appendix A, this spreadsheet has the advantage of being set up for the discrete lamina thicknesses used to build actual parts. It also has the benefit of having successfully sized, and verified through proof testing, many struts of this type in the past. As such, it was used by Park to size the strut that was eventually built. A version of this spreadsheet with the as-built input and results can be found in Appendix B.

ABAQUS Analysis of 110K Strut

The closed-form analysis of Appendix A used for performing sensitivity studies had the advantage of allowing rapid preliminary design-level sizing. It was, however, not detailed enough to examine all aspects of interest for the sizing of these composite struts. To fill in that analytical gap, a series of ABAQUS models was developed.

The first finite element model (FEM) models the entire strut in a simplified manner by imposing two planes of symmetry. This model also integrated a representation of the end-fitting with its undulations. A graphic representation is shown in Figure 21.

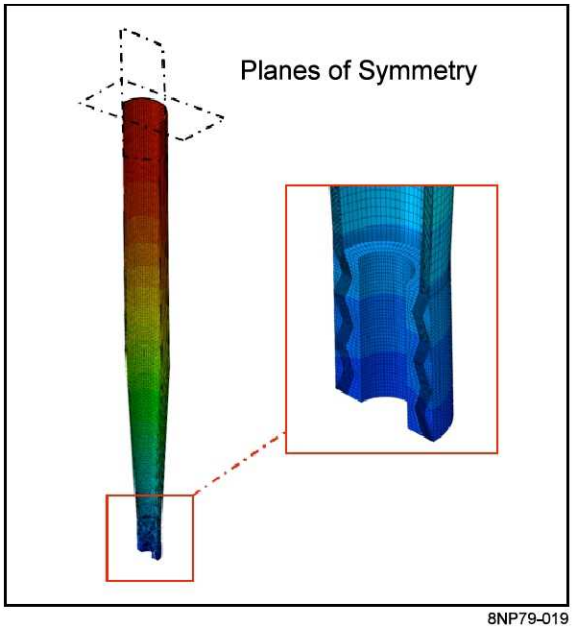

Figure 21. ABAQUS Model of the 110 kip Strut

One key area in which this model provides increased fidelity is at the intersection of the constant section and the beginning of the end tapers. Here the intersection of conical and cylindrical shells gives rise to local discontinuity moments, stresses and strains. These axial and hoop strain gradients are not captured in the closed-form sizing approach but can clearly be seen in the ABAQUS results of Figure 22.

A review of these strains in Figure 22 at the 110 kip ultimate load level clearly indicates that the laminate loading is well within its strain allowables. Furthermore it implies that it is reasonable to assume, at least for preliminary design, that the midspan strength sizing dominates and that this secondary effect can be ignored for preliminary sizing and sensitivity studies.

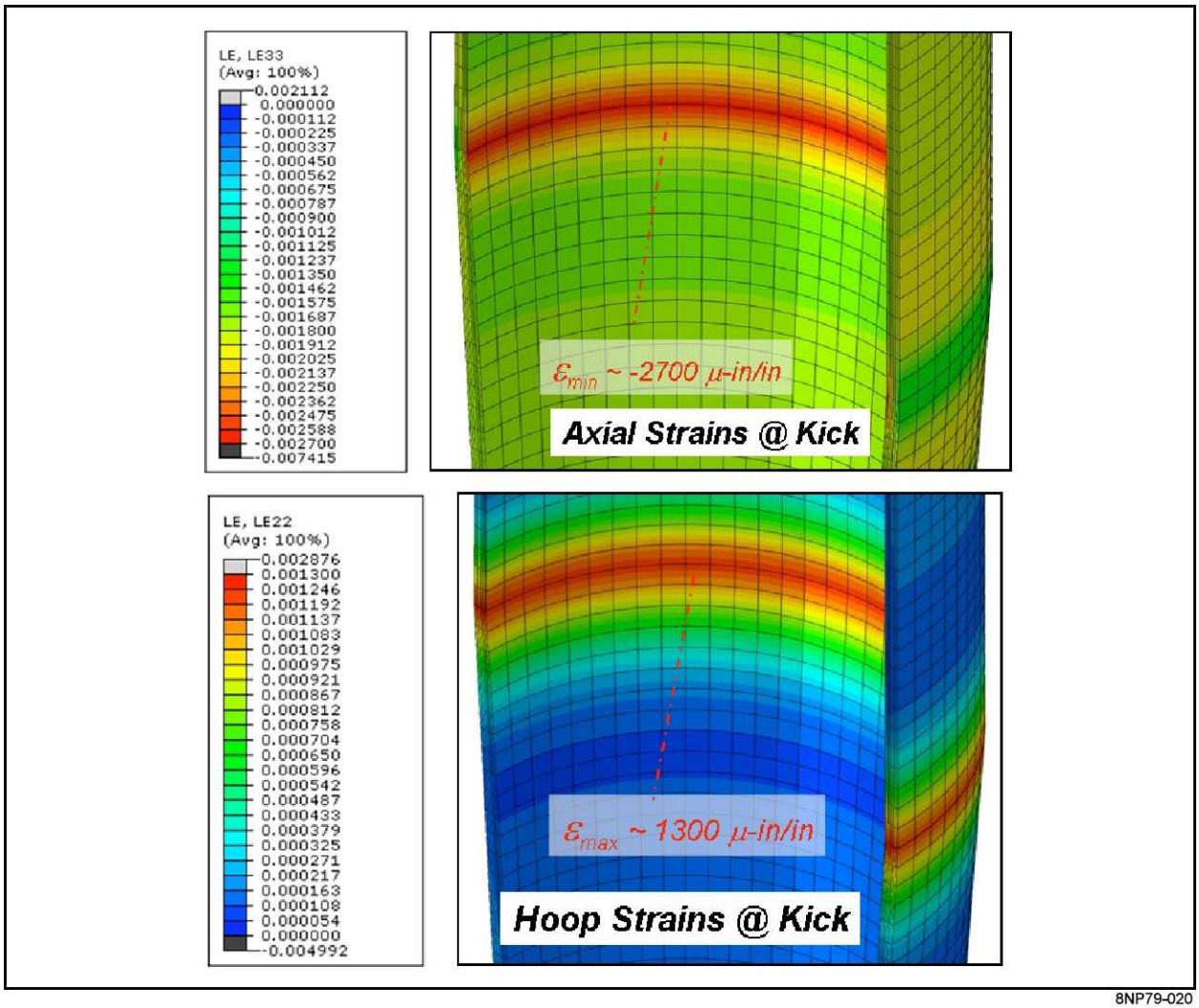

Figure 22. Axial and Hoop Strains at Transition From Conical to Cylindrical Portion of the Strut

The initial intent was to use this model to examine interaction between the metallic end fitting and the composite strut as well. However, as the analysis progressed, it was decided that a dedicated, higher-fidelity, axisymmetric FEM be developed to study that interface. This axisymmetric FEM is shown in Figure 23. Notice the refinement of the mesh of the hoop (light blue) plies in Figure 23.

One interesting insight from the results of this model was the distribution of the axial load between the composite strut and successive end-fitting "ramps." The fringe plot of Figure 24 depicts the variation in hoop ply strains along the length of the metallic fitting-to-composite strut joint.

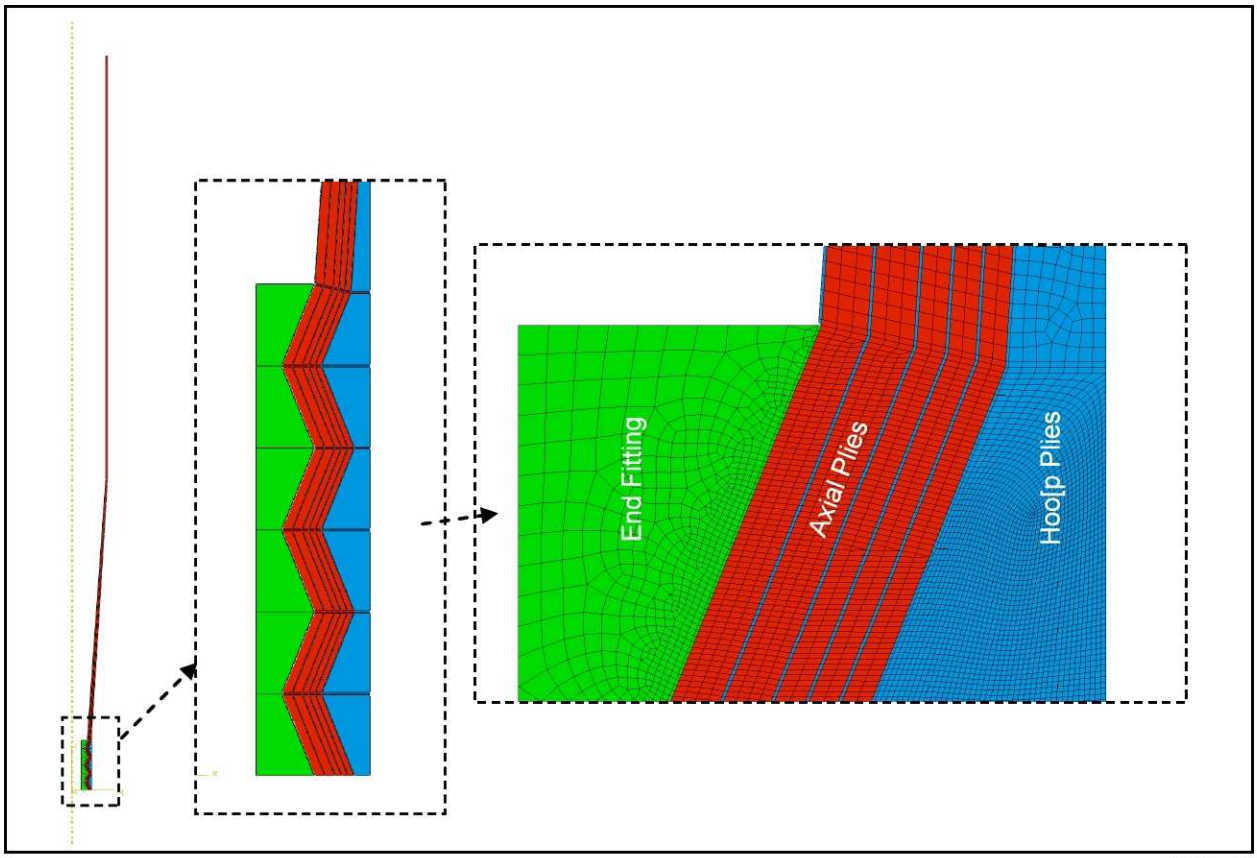

Figure 23. Axisymmetric ABAQUS FEM

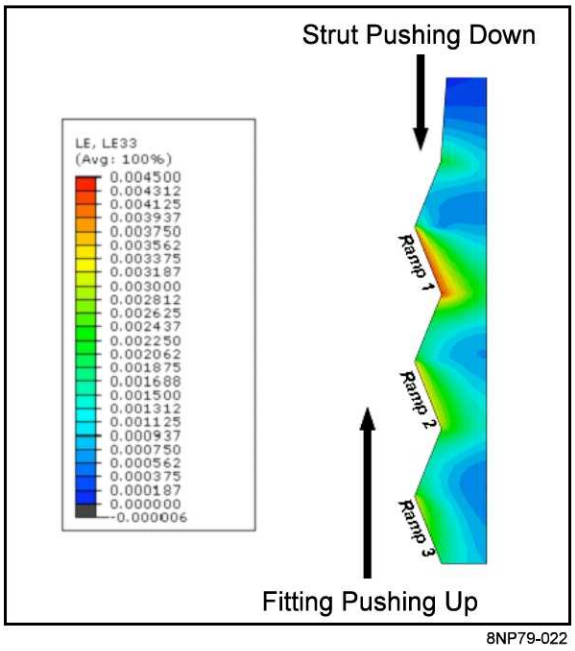

Figure 24. Variation in Hoop Ply Strains Along the Length of the Metallic Fitting to Composite Strut Joint

Clearly the zone of influence around ramp 1 is much larger, with significantly higher strain levels, than for either ramp 2 or 3, indicating a greater amount of load transfer. Similarly ramp 2 is more highly loaded than ramp 3. Examination of these strains, mixed with some judgment, indicates that the load distribution shown in Figure 25 is a reasonable assessment of how this load transfer varies from ramp to ramp. This is the distribution that was used as input in the sensitivity sizing spreadsheet described in Appendix A.

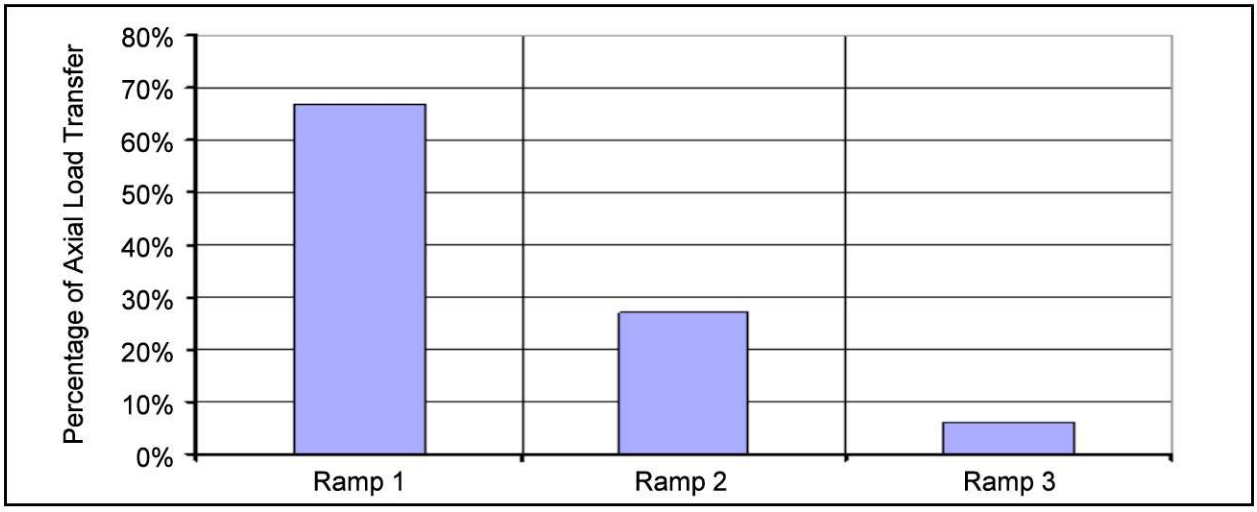

Figure 25. Ramp Load Distribution for Strut Under 110 kip Compressive Load

The drastic dropoff in load transfer between the first and subsequent ramps indicates that weight savings may be possible by either eliminating the third ramp, reducing the amount of overwrap plies as the end of the fitting is approached or both. This may not amount to much of a weight savings on a highly loaded strut like this but could lead to some appreciable savings for lightly loaded struts.

MANUFACTURING METHODOLOGY

Overview

The manufacturing demonstration article fabricated as a part of this study was a 127-inch-long, 6-inch diameter strut designed to carry 110 kips of axial compression. The design calculations are shown in the spreadsheet provided in Appendix B. The strut was fabricated by Park Aerospace Structures Corporation of Lynwood, Washington, using their patented manufacturing process. The strut concept uses a unique metal end fitting (patent pending) that is cocured into each end of the strut without the use of adhesives. Through a combination of hand lay-up and filament winding, the end fittings are structurally cocured into place. The manufacturing sequence is illustrated in Figure 26 and described in detail with respect to the demonstration strut fabrication activities in the following paragraphs. In summary, the process consists of casting a strut IML mandrel on a steel core to maintain colinearity, sliding the end fittings over the steel core to butt against the mandrel, first hand laying a set of 0-degree plies over the fitting and the mandrel followed by filament winding 90-degree plies, and then repeating the process until the design lamina sequence is achieved. After a suitable cure process, the steel rod is removed and the IML mandrel washed away to yield the final part. This end fitting embedment process allows the fittings to carry the full strut body design ultimate load without having to rely on large-bond areas to carry shear loads as is typical in other current designs. The end fittings are bored out and threaded internally to receive a metal rod end attachment or other threaded end pieces such as those shown in Figures 19 and 20.

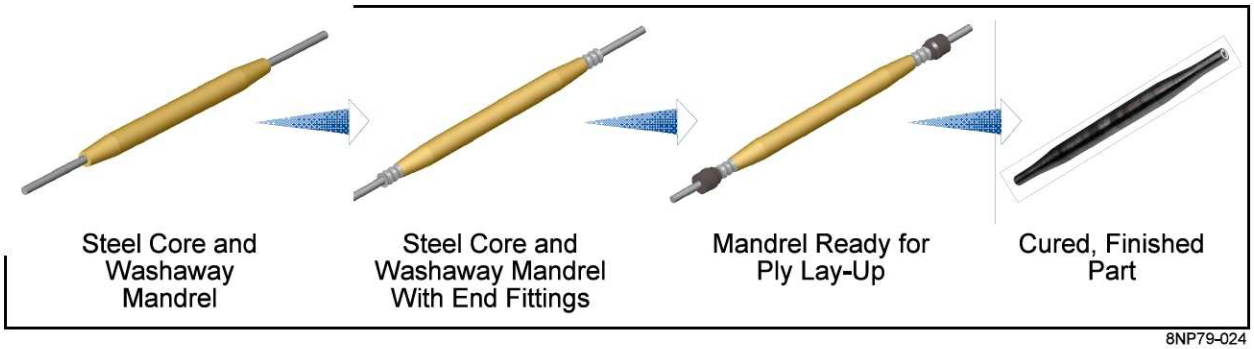

Figure 26. Strut Manufacturing Sequence

Process Description for 110 kip Strut Manufacture

The manufacturing process used was: (1) a molded washout plaster mandrel was cast about a steel centering support rod, (2) the mandrel was wrapped with Teflon tape then the 0-degree and 90-degree plies were hand laid up and filament wound, respectively to achieve a lay-up sequence of $[90/0_3/90/0_3/90/0_2/90/0_2/90/0_2/90]$, (3) the strut was wrapped in shrink tape then vacuum oven cured, and (4) tooling was washed out with water, the Teflon tape removed with forceps and the ends ground flat and parallel. The finished strut ready for shipment is shown in Figure 27. Details of the manufacturing process are presented in the final report for National Aeronautics and Space Administration (NASA) Contract NNL04AA13B Task Order: NNL08AC95T.

Figure 27. SETS demonstrator strut

The strut was nondestructively inspected for defects using ultrasonic A-scans. The only signal reflections obtained were in the tapered areas where the tows and the slit tape have to be locally folded over to accommodate the excess material as the cross section narrows. No inspection standards were available, and no cross-section cutaways could be obtained without damaging the strut.

CONCLUSIONS AND RECOMMENDATIONS FOR FUTURE WORK

Conclusions

A 127-inch-long strut capable of carrying 110 kip compression loading representative of lunar lander truss structures loading was designed, analyzed for margins, fabricated, and delivered to NASA Langley Research Center (LaRC). Sensitivity studies were conducted to identify design drivers and strategies for optimum strut design. In the class of carbon fiber/epoxy matrix struts considered, the competing failure modes were overall Euler buckling of the strut, local composite strut wall buckling, and strength rupture of the strut in compression. For both struts, an 80 percent 0-degree, 10 percent 45-degree, and 10 percent 90-degree ply lay-up resulted in the lowest weight. Further, for the two struts considered, a 7-inch-diameter construction yielded minimum weight. The lightly loaded strut benefited from the use of a high-modulus M55J class of fibers. For both struts, damage-tolerance allowables had to be reasonably selected since they are tremendously reduced for lay-ups that do not have any 45-degree plies. Magnitude of the initial bow in the strut was also a strong driver of the strut weight. A comprehensive closed-form design methodology was developed for sizing and optimizing carbon/epoxy struts subjected to high loads.

The manufacturing demonstrator showed that even for long struts the central bow in the strut can be controlled by suitable tooling design. The characteristic bow obtained with the demonstrator strut was 0.1 inch, which is less than 1 percent of the part length. All the process details, such as 90-degree ply wrapping, shrink tape debulking, and multiple cures, to name a few, are quite mature and resulted in a perfect strut.

Recommendations for Future Work

A primary recommendation for future work is to perform static tests on the struts to validate the design process and the integrity of the strut. Prior to practical applications, a truss "building block" test program needs to be performed that includes validation of joint fittings at ends, and verification of predictive capability of the truss load carrying capacity in relevant environments that may include vibratory and acoustic loads and relevant damage-tolerance allowables. Struts capable of carrying compression as well as substantial tension load also need to be designed, fabricated, and tested.

APPENDIX A
Closed-Form Analysis Methods and Intermediate Calculations

Overview

An Excel spreadsheet was developed to perform rapid, preliminary design-level fidelity sizing of tapered cylindrical composite struts. This tool allows minimum weight sizings to be quickly determined for a variety of materials, lay-ups, geometries, and load levels. It was used to study the sensitivity of total strut weight to variations in key input parameters.

Spreadsheet Setup

The sizing spreadsheet is comprised of nine tabs with the "Sizing" tab being the driver. All pertinent information is input here, and it is the only tab requiring modification to vary the configuration being sized. The other tabs either provide necessary material data or perform one specific type of calculation and have the information necessary for its operation supplied to it from the "Sizing" tab.

Each number in all tabs is either blue, red, or black with its color indicating the nature of that number. Blue values are input and are required to define the problem, red numbers are calculated values, and black values have been input or computed elsewhere and have been transferred to the current cell. Red and black numbers should not be touched. Some numbers are bold and/or appear in colored boxes; these indicate values of particular importance but otherwise still follow the blue, red, and black designation rules.

The following sections describe the individual tabs in detail as well as provide tips for their use. In many cases copies of the pertinent methodology being used has been embedded in the tab itself. Scroll down and/or right to find it.

"Sizing" Tab

Again the data entered on this tab drives the entire sizing analysis, and the results presented summarize the key results. As such no other tabs need be examined/modified in order to perform a variety of strut sizing analyses/sensitivity studies.

There are six basic sets of input that are required to define the sizing analysis. The first is the applied load. The following pieces of information are required;

- Applied load @ limit
- Factor of safety
- Temperature.

Currently, the material data is limited to *only* temperatures in the 70°F to 113°F range. Material data, and more importantly the material allowables, are linearly interpolated for temperatures in between. Use of temperatures outside of this range will cause the program to extrapolate and may lead to unconservative results.

Next, the overall strut geometry must be input. Figure A-1 depicts the key strut dimensions. Only the dimensions in blue need be provided as input and not all of them at the beginning of the analysis process. The other geometric properties will be computed as part of the analysis. There

is one more very important geometric parameter that must be input – the initial midspan deflection (i.e., imperfection).

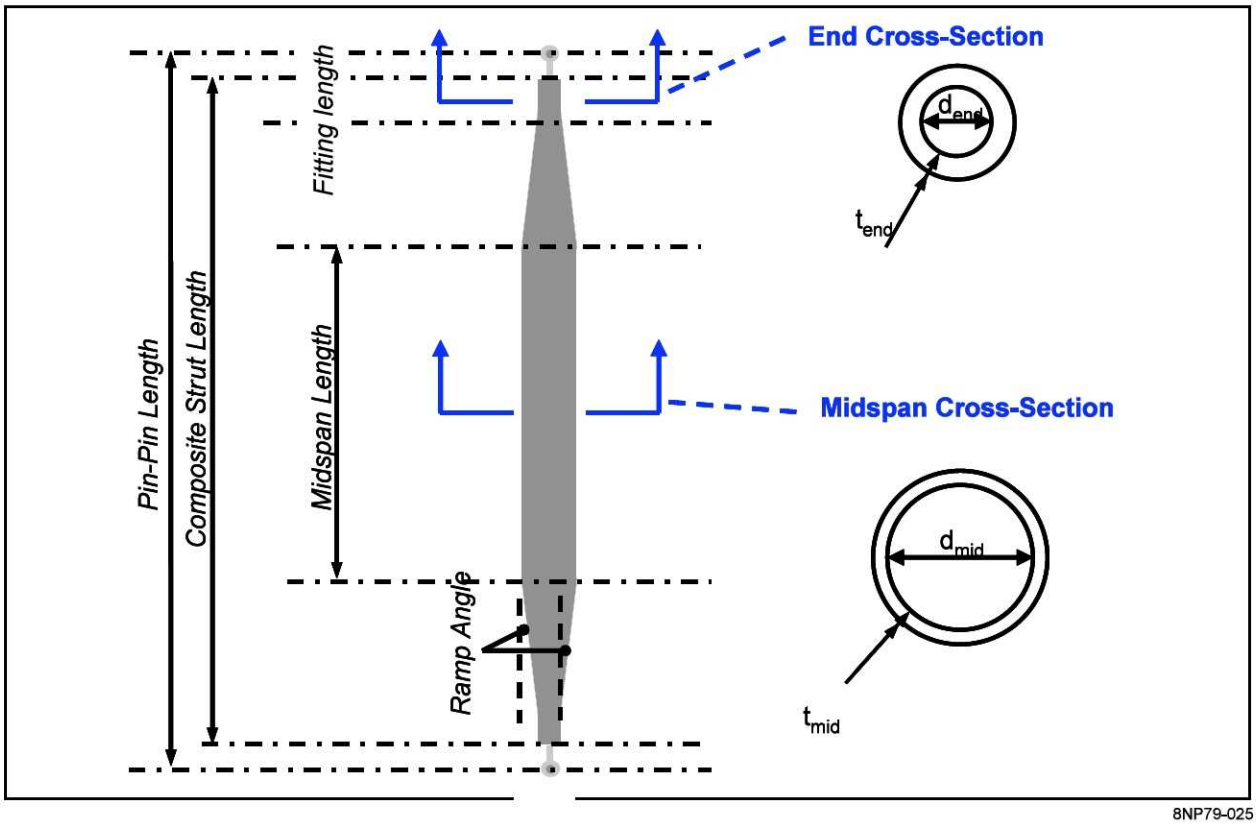

Figure A-1. Key Strut Dimensions

Several key assumptions are currently buried in the computations in order to complete the definition of the geometry. The first is that the distance between the end of the composite strut and the centerline of the attachment pin is approximately 2 inches. Therefore the composite strut length is assumed to be the pin-to-pin length minus 4 inches. Alternate fitting lengths can be accommodated by directly inputting both the pin-to-pin and composite strut lengths. The other key assumption is that the strut's cross-sectional area remains constant along the entire length. This means that the thickness increases as the diameter decreases along the end tapers.

The next set of required input parameters defines the end-fitting and its load distribution characteristics. The fitting geometry is depicted in Figure A-2.

Overall length, inner and outer radii, ramp angle, the number of ramps (the default is six), and the fitting weight need to be provided as input. In addition, the distribution of axial load transfer between the three successive effective ramps (see "End Overwraps" tab) must be input. The factor for the first ramp is assumed to be 1.0. The factors for the second and third ramps are defined as follows;

β = load transferred by second ramp/load transferred by first ramp

γ = load transferred by third ramp/load transferred by first ramp

Again, the current code is hardwired for three effective ramps. Also note that using this definition the total of $(1 + \gamma + \beta)$ does *not* equal one.

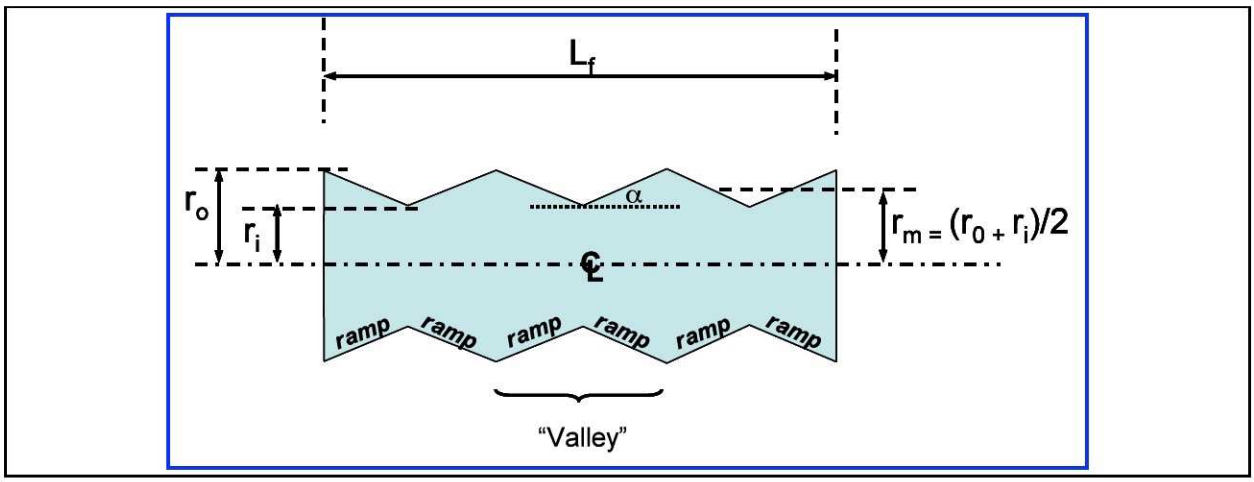

Figure A-2. End-Fitting Geometry Characterization

Defining the material properties is relatively simple. This is done by entering one of the following three names "AS4," "IM7," or "M55J," which designates the fiber to be used in the analysis. This name, the design temperature, and ply percentage distribution is forwarded to the "Material Properties" tab. There the lamina stiffness properties are extracted, the strain allowables are computed, and the results are sent back to the "Sizing" tab. Care must be taken to correctly spell AS4 or IM7 as the program defaults to M55J properties if it does not recognize the material title.

Along with the lamina material, some description of the lay-up must be provided in order to fully define the laminate. In a detailed design analysis, this is done by providing the number of plies, the per-ply thickness, ply orientation, and the ply stacking sequence. This provides a complete description of the laminate and, by means of lamination theory, its stiffness properties. However, this takes a prohibitive amount of input for performing the rapid sizing turnaround needed for performing sensitivity studies. Therefore, a simplified approach was adopted.

A ply orientation percentage distribution is input by defining what *percentage* of four-ply orientations should be present in the laminate. Combining this with the laminate thickness (provided as an input later), the thickness of each of the four ply orientations can be derived. The ply percentage distribution and overall laminate thickness is forwarded to the "Laminate" tab where the laminate axial and bending stiffness parameters are computed.

Currently the code can accept any four values of ply orientation, but the program as a whole is geared towards looking at 0-, +45-, -45-, and 90-degree laminate families. Care must be taken if the user deviates from this. In particular, the allowables derivation method, which is currently predicated on the total percentage of 45-degree plies, must be re-evaluated if other laminate families are used in this analysis. Also, it is obviously important to make sure the sum of the percentage of the four-ply angles equals 100 percent.

Once the aforementioned information is input, the sizing analysis can proceed. The analysis is performed by first entering the laminate thickness (cell C42) and end overwrap ply thickness (cell C48) and allowing the code to compute the following five margins:

- Euler buckling
- Local buckling
- Compressive strain at midspan
- Interlaminar shear stress at the kick
- Overwrap ply strains.

These are reported under the Analysis Summary heading. An acceptable, and minimum weight, solution can be found by performing a series of "goal seek" operations in which a negative margin is selected, has its goal set to zero, identifies one of the two input thicknesses as the variable, and then generates an updated thickness. This process continues until the minimum margin is 0.00 and all the other margins are positive and as low as practically possible (some judgment is needed here). The resulting strut weight (basic strut + end overwraps + fittings) is computed and presented in cell H54.

There are several things to keep in mind while iterating to a minimum weight solution. First, the Euler margin can never be zero for a column with an initial eccentricity (see "Eccentricity" tab). However, a good approach for getting relatively close is to first goal seek for a zero Euler margin, which will result in negative strain and/or local buckling margins, then goal seek the more negative of these to zero, and then goal seek the other to zero if required. Interlaminar shear stress does not seem to be a driver for these configurations. All of these operations are performed using the strut laminate thickness as the variable. Lastly, the overwrap ply margin needs to be corrected (made positive or minimized) by goal seeking on this margin using the overwrap ply thickness as the independent variable. There is a very weak interaction between the laminate and overwrap thickness so, to obtain an absolute minimum, the user might wish to repeat several steps while monitoring the weight to verify that a minimum weight has been reached.

Finally, at the bottom of the analysis summary, a few analysis integrity checks are made. The first, in cell C59, checks to make sure the applied load does not exceed the Euler critical load. If it does, the local buckling and compressive strain margins computed are erroneous (of course, checking to make sure that the Euler margin of safety (MS) is greater than zero does the same thing). The second, located in cell C60, verifies that the sum of the percentage in the laminate definition equals 100 percent. The user should make sure that these flags do not indicate any problems before using the results.

"Local Buckling" Tab

This tab uses the local buckling methodology* defined in Reference 2 to determine the critical compressive running loads for a cylinder under axial load and bending. This methodology, and the definitions of the cylinder bending stiffness parameters from Reference 3, are included in this tab (scroll right) for quick reference.

The key equation for computing the critical axial running load is:

$$\frac{N_x \ell^2}{\pi^2 \overline{D}_x} = m^2 \left(1 + 2 \frac{\overline{D}_{xy}}{\overline{D}_x} \beta^2 + \frac{\overline{D}_y}{\overline{D}_x} \beta^4 \right) + \frac{\gamma^2 \ell^4}{\pi^4 m^2 \overline{D}_x r^2} \frac{\overline{E}_x \overline{E}_y - \overline{E}_{xy}^2}{\overline{E}_x + \left(\frac{\overline{E}_x \overline{E}_y - \overline{E}_{xy}^2}{\overline{G}_{xy}} - 2\overline{E}_{xy} \right) \beta^2 + \overline{E}_y \beta^4}$$

Equation A-1

where Nx is the axial running load at buckling; Es, Ds, and Gs are cylinder stiffness parameters; β is the buckling ratio parameter (nl/πrm); and γ is a parameter that accounts for initial cylinder wall imperfections. This same equation applies to both axial load and bending with only the initial imperfection parameters, γ, varying.

Reference 3 provides the following γ parameters

$$\gamma = 1 - 0.901(1 - e^{-\phi}) \text{ for axial}$$

$$\gamma = 1 - 0.731(1 - e^{-\phi}) \text{ for bending}$$

and the following equation for computing ϕ

$$\phi = \frac{1}{29.8} \left[\frac{r}{4\sqrt{\frac{\overline{D}_x \overline{D}_y}{\overline{E}_x \overline{E}_y}}} \right]^{\frac{1}{2}}$$

Equation A-2

The buckling Nx equation and the β factor as well are both a function of the presumed buckled shape. This shape is defined by the number of half buckle waves in the axial direction (m) and the number of waves in the circumferential direction (n). As such this equation only provides the *critical* Nx value if the *critical* combination of n and m is inserted.

The spreadsheet determines the critical value for Nx by computing the Nx for *all* combinations of m = 1 to 50 and n = 1 to 50 and by searching for the resulting minimum magnitude. This is done for both axial load and bending with the resulting Nx critical values being identified. Ratios of the applied Nx to the allowable Nx values are computed for both axial and bending with the two being linearly combined (i.e., added) to obtain the total critical load ratio (R). The local buckling margin of safety is then computed as (1/R) -1. The resulting local buckling MS is then returned to the "Sizing" tab.

* NOTE: This reference provides an alternate, more cumbersome, method of developing the buckling Nx, again as a function of the assumed m and n values:

$$N_x = \left(\frac{\ell}{m\pi}\right)^2 \frac{\begin{vmatrix} A_{11} & A_{12} & A_{13} \\ A_{21} & A_{22} & A_{23} \\ A_{31} & A_{32} & A_{33} \end{vmatrix}}{\begin{vmatrix} A_{11} & A_{12} \\ A_{21} & A_{22} \end{vmatrix}} for(n \geq 4)$$ Equation A-3

Comparison of results made using this approach with those derived using the equation in Reference 3 showed a good match at lower values of m and n but diverged slightly at higher values of these parameters. However, if the factor of 2 is replaced with a factor of 1 (as seen by the red correction shown in Equation A-1), the difference between the values predicted by these two methods disappears. Consequently, it is believed that there is an error in the referenced equation and the "corrected" version, i.e., using the factor of 1, was used here.

ILS @ Kick" Tab

This tab makes an interlaminar shear (ILS) stress check where the constant cross section begins to taper. The following formula is used for making this check;

$$f_v = \left(\frac{3}{2}\right)\left(\frac{P * tan(\beta)}{\pi dt}\right)$$ Equation A-4

where

P = total axial load

β = taper angle

d = mean diameter at start of taper

t = laminate thickness at start of taper.

The resulting interlaminar shear stress is compared to the ILS allowable, and a margin is written. Because the cross sectional area is held constant along the entire taper, resulting in a constant d * t, this check is applicable to both ends of the taper.

"Laminate" Tab

This tab takes the percentage ply angle distributions and thickness provided on the "Sizing" tab and, using classic lamination theory (see Reference 4), develops lay-up-independent laminate axial and bending stiffness parameters. Specifically it computes E_x, E_y, ν_{xy}, G_{xy} , D_{11}, D_{22}, D_{12}, and D_{66} and returns these values to the driver tab. The bending stiffness parameters are computed using the axial properties and the thickness – rather than using the lamination theory directly – in order to eliminate the influence of ply stackup. Including this influence would considerably complicate the resizing process, and its inclusion was not considered critical for the first-order sizing used in sensitivity study analyses.

"Eccentricity" Tab

This tab performs the computations required to account for the fact that, in all likelihood, the as-built strut will not be perfectly straight. While there are probably an infinite variety of potential initial imperfections, a reasonably representative one, an initial sinusoidal shape with the maximum offset located midspan, will be assumed here. This is shown graphically in Figure A-3.

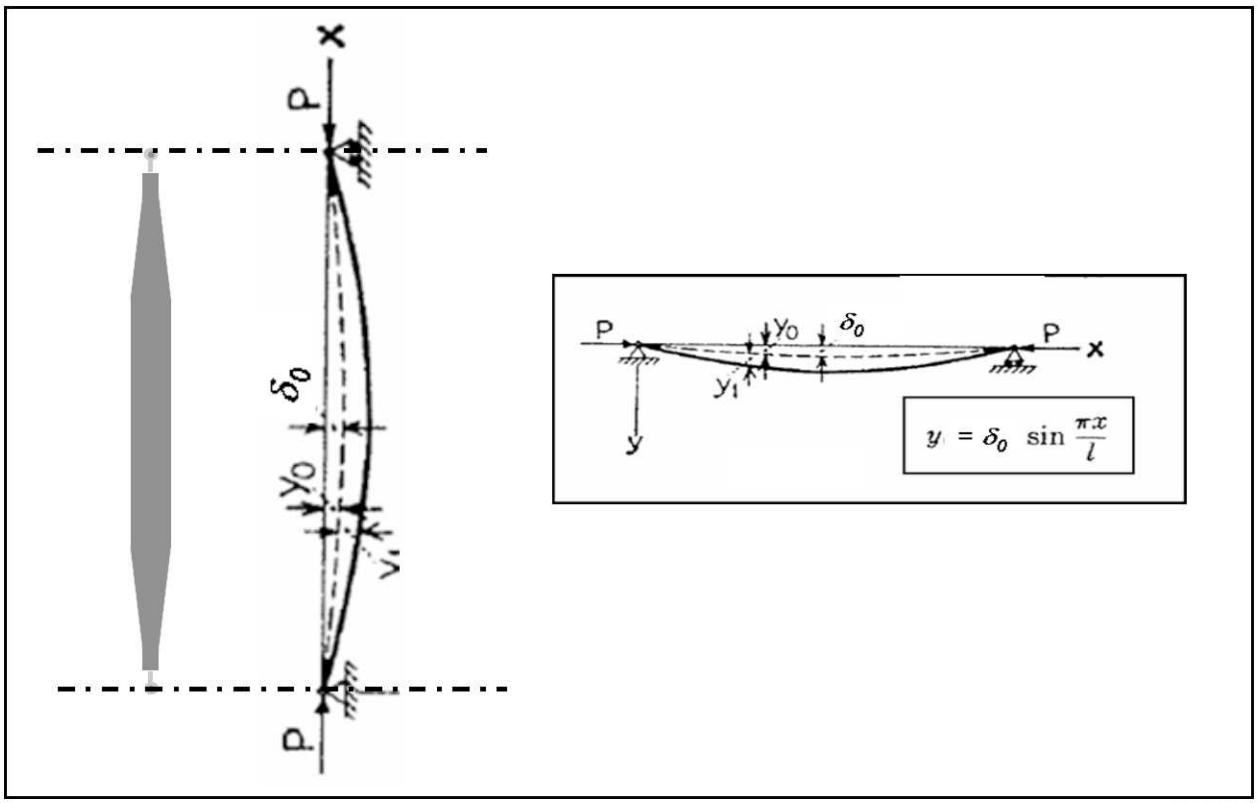

Figure A-3. Beam Column Analysis for Buckling Load Prediction With Initial Imperfections

In accordance with the methodology described in Reference 5, this midspan eccentricity becomes progressively larger with increasing compressive load level while the overall deflection maintains a sinusoidal shape. The relationship for computing the loaded midspan offset from the initial offset and the applied load is;

$$\delta = \frac{a}{1 - P / P_{cr}} \qquad \text{Equation A-5}$$

where

P = applied axial load

P_{cr} = Euler buckling load

δ = total midspan deflection

a = initial midspan offset (imperfection).

The midspan offset gives rise to a midspan moment equal to the applied axial load * δ. This moment produces additional stresses and strains that must be superimposed on those resulting from the straight axial load. The total resulting stresses may be computed as follows:

$$\sigma_{max} = \frac{P}{A}\left(1 + \frac{a}{s}\frac{1}{1 - P/P_{cr}}\right) \qquad \text{Equation A-6}$$

where

P = applied axial load

P_{cr} = Euler buckling load

A = cross-sectional area at midspan

I = cross-sectional moment of inertia at midspan

r = outer radius at midspan

a = initial midspan offset (imperfection)

s = I/(rA).

The associated critical compressive strain is computed by dividing σ_{max} by E, and the related critical axial load and bending induced running loads are computed by multiplying by the wall thickness.

An important inference from these equations is that the midspan deflection, and the associated bending moment, increase rapidly as the applied axial load approaches the critical Euler value. Consequently, a positive Euler buckling margin must be maintained to preclude an infinite midspan bending moment from developing. In other words the critical failure mode can never be Euler buckling for a column that is not perfectly straight.

This tab gathers the necessary data and computes the midspan deflection and the axial and bending-induced critical running loads as well as the compressive strain strength and Euler buckling margins. These MSs are returned to the "Sizing" tab while the critical running loads are forwarded to the "Local Buckling" tab for local cylinder stability checks.

"Material Properties" Tab

This tab provides the material property data and computes the allowables for the three materials under consideration in this study: IM7, AS4, and M55J tape impregnated in epoxy resin. This tab does include blue (i.e., input) values that are needed to perform the analyses. However, these have already been included and should not be changed from sizing to sizing *unless* this database needs updating.

This tab takes the name of the material being considered from the "Sizing" tab and matches it with the appropriate database in this tab. *Care must be taken* to use only one of the three following material names – AS4, IM7, or M55J. The code will automatically and potentially incorrectly default to M55J if AS4 or IM7 are misspelled.

Once the proper database is identified, this tab used the percentage of all the plies that are not 0 or 90 (i.e., typically the amount of 45s) to compute the strain allowables for the specified lay-

up. It computes these for both room temperature dry (RTD) and 113°F wet and returns these values to the "Sizing" tab for future computations.

The values provided in this tab are based on 0.25-inch open-holed specimens and, as such, take into consideration damage tolerance. These should not be confused with "pristine" allowables, which do not consider damage tolerance. In general these "damaged" allowables should be used for strut sizing.

"Material Properties Pristine" Tab

This tab performs the same function and provides the same data that the basic "Material Properties" tab provides. However, the data included here does *not* account for any damage that may be encountered during fabrication and/or use. Typically these are not used in sizing real-world struts. It has been included here to allow the performance of sensitivity studies of the weight penalty suffered by imposing damage-tolerance criteria.

The baseline sizing spreadsheets do not use this for the basic strut sizing, and as such, their "Sizing" tab does not point to this tab. In order to use these pristine allowables the "Sizing" tab needs to be adjusted to point to this tab for extracting the lamina data. In cases in which this was needed, special spreadsheets annotated "Pristine" have been developed. Consequently care must be taken to make sure the version of the spreadsheet being used calls the appropriate/intended material data.

"Tapered Column" Tab

This tab computes the critical Euler buckling load for a tapered pin ended column. Essentially the basic Euler column capability of

$$P_{crit} = \left(\frac{\pi}{L}\right)^2 EI \qquad \text{Equation A-7}$$

is computed, using the EI at the small ends of the tapers, and then adjusted by a factor that accounts for the tapering. This modification factor is developed using methodology obtained in Reference 6 with the pertinent graph included in the tab. This graph provides curves of adjustment factor "m" as a function of the ratio of the moment of inertia at both ends of the taper for a variety of constant cross-section length to overall length (a/L) ratios.

These curves have been curve fit to enable the spreadsheet to numerically manipulate the data to derive an "m" factor instead of having to manually pick the appropriate value off the chart and enter it into the code for each analysis. It does so by computing the "m" value for the given I ratio for all a/L ratios and linearly interpolates between the two curves bounding the given a/L. The basic Euler P_{crit} value is divided by the derived "m" factor to obtain the tapered column P_{crit}.

In performing these computations, certain assumptions were made. First, the a/L value is computed using the length of just the strut itself, i.e., it does not include the length of the end-fittings. Conversely, the computation of the Euler buckling value uses the entire pin-to-pin length. The program also computes the basic Euler P_{crit} assuming no taper and the constant cross-section EI value and the ratio of the adjusted and not adjusted values to get a feel for how much the taper is impacting overall stability. These comparison values are not used in any subsequent computation but are available for reference.

"End Overwraps" Tab

This tab sizes the overwrap required to prevent the composite strut from separating from the undulating metallic fitting. There are several underlying assumptions in these computations. First, it is assumed that all load is transferred between the fitting and the composite strut in bearing and that only the "ramps" in compression are effective in transferring this load. This is illustrated in Figure A-4.

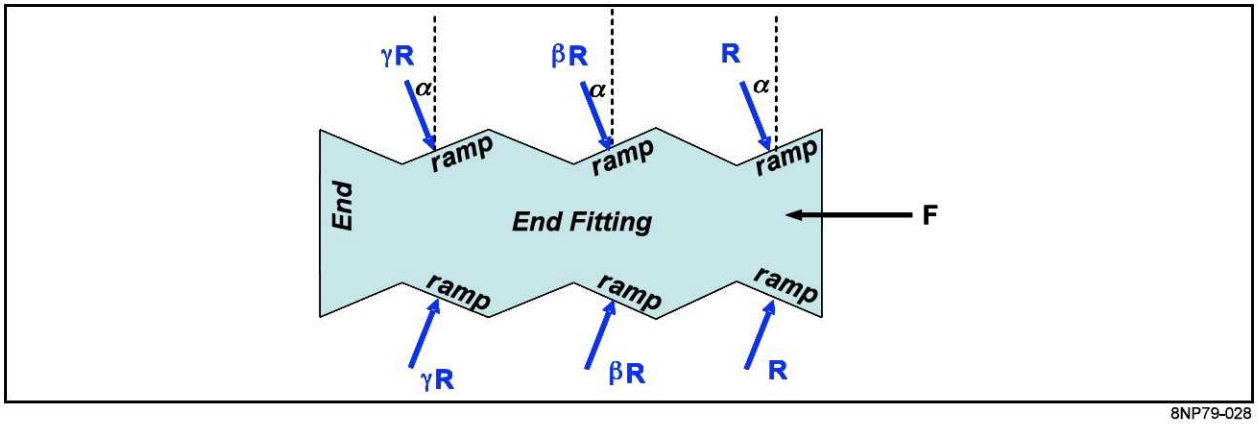

Figure A-4. Geometry for Radial Stresses in Hoop Wraps

Furthermore, it is assumed that each ramp is not equally effective but that the "first" ramp (i.e., farthest from the end) takes a higher proportion of the total load with each successive ramp taking less. Consequently the equation for transferring the total strut force F would be:

$$F = (1 + \gamma + \beta)R \qquad \text{Equation A-8}$$

The radial (i.e., R) loads are the summation of the radial pressure produced when the special end overlay plies, i.e., circumferential or "hoop" plies, are stretched. These dedicated 90 plies are wound around the fitting for this express purpose. Consequently, there must be enough of these to be able to develop the required constraining hoop pressures without being overloaded themselves. The equation used to determine the critical hoop ply strains is as follows:

$$\varepsilon_{hoop} = \frac{F * n * \left(r_m + \frac{t}{2}\right)}{(1 + \gamma + \beta) * (\tan\alpha) * (\pi r_m L_f) * Et} \qquad \text{Equation A-9}$$

where

F = total axial load

r_m = mean radius

n = number of "valleys" in the fitting = number of effective ramps, (Figure A-4 configuration = 3)

t = thickness of the hoop plies

E = hoop ply modulus

L_f = overall fitting length

γ and β = relative ramp load distribution factors.

Using this equation, this tab computes the hoop ply strains and compares this to the *pristine* allowables to determine a hoop ply margin. This margin is then returned to the "Sizing" tab.

There are several reasons why the pristine allowables was used here instead of one that considers a knockdown caused by damage. First, these are applied over a relatively small area and not as prone to damage. Next, dropping a heavy object on these plies, which are already circumferentially wound around a metallic fitting, would not produce nearly the amount of damage that you would see if you hit the thin sidewall at midspan; consequently, the use of the same open-hole values at both locations seems overly conservative. Lastly, there is a sizable amount of 90-degree plies wound onto the ends to fill in the valleys before the 90-degree plies being sized here are applied. These are not considered in the overlay sizing calculation, and not doing so is conservative.

For a clearer understanding of analysis performed in this tab, several comments/assumptions should be mentioned. First, it is set up under the assumption that the fitting has three (or less) valleys. The spreadsheet would have to be adjusted if additional valley were to be considered effective (which is not likely). Second, these 90-degree plies are added on top of those already in place from the basic strut laminate. These basic plies are assumed to contribute to the hoop loads being developed and are included in the computation. Finally, it is important to understand that the resulting weight associated with these additional overwrap plies is relatively small so any small errors embedded in these calculations would have an insignificant impact on the sensitivity studies for which this spreadsheet is intended to be used.

The embedded spreadsheets below show all the calculations conducted for the design of the two struts and the sensitivity studies. A spreadsheet with a summary of the sensitivity results is also embedded below and includes figures – most of which were shown in the main body of the text.

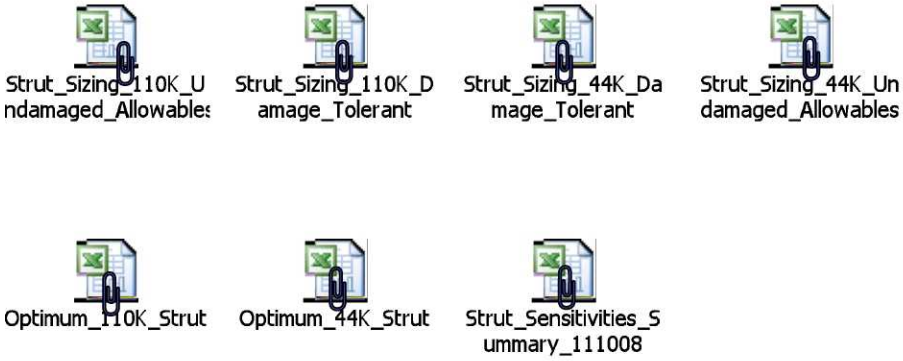

APPENDIX B
Park Aerospace Corporation Design Calculations

Park's strut sizing spreadsheet, which was used to size the manufactured strut, is included here. The various boxes are colored coded to define which values require input (light blue), which require some sort of midanalysis check (red), and those with values that have been visually examined and shown to be good (light green).


Park Aerospace 110
kip Design Worksheet

One important thing to understand about this spreadsheet is that it has several important parameters and assumptions hard coded into it. For example, per-ply thickness for 0-degree plies is taken to be 0.0123 inch, and for 90-degree plies it is 0.0051 inch. The spreadsheet as currently written does not accept any 45-degree plies. Furthermore, the allowables incorporated in the spreadsheet are: tension strain, 7,500 μ-in/in; compression strain, -5,000 μ-in/in; interlaminar shear stress, 6,000 psi; and hoop ply tension allowable, 100 ksi. These values are empirically derived based on Park's experience and are consistent with IM7 fibers with some level of damage tolerance taken into account. This spreadsheet would need to be modified for applications in which variables such as lay-up families, fiber types, and allowables were to be changed.

REFERENCES

1. McLaughlin, M., Palm, T., Berry, J., "Structures and Mechanisms for Max Launch Abort System for the Orion Crew Module", NASA LaRC Contract NNL07AE35T.
2. NASA, "Buckling of Thin Walled Circular Cylinders," NASA SP-8007, August 1968.
3. Timoshenko, S., Woinowsky-Krieger, S., "Theory of Plates and Shells," Second Edition, McGraw-Hill Book Company, New York, 1959.
4. Northrop Grumman, "Advanced Composites Structures Manual," First Draft, 1995
5. Timoshenko, Stephen P., "Theory of Elastic Stability," Second Edition, McGraw-Hill Book Company, New York, 1961.
6. Northrop Advanced Systems Division, "Structural Design Manual," EAA1312-005, January 1984.

REPORT DOCUMENTATION PAGE

Form Approved
OMB No. 0704-0188

1. REPORT DATE *(DD-MM-YYYY)*	2. REPORT TYPE	3. DATES COVERED *(From - To)*
01-05-2010	Contractor Report	

4. TITLE AND SUBTITLE
Design of Structurally Efficient Tapered Struts (SETS)

5a. CONTRACT NUMBER
NNL04AA13B

5b. GRANT NUMBER

5c. PROGRAM ELEMENT NUMBER

6. AUTHOR(S)
Deo, Ravi; Benner, Harry; Dawson, Vincent; Olason, Eric; Harrison, Richard

5d. PROJECT NUMBER

5e. TASK NUMBER
NNL08AC95T

5f. WORK UNIT NUMBER
727950.04.05.23

7. PERFORMING ORGANIZATION NAME(S) AND ADDRESS(ES)
NASA Langley Research Center
Hampton, VA 23681-2199

8. PERFORMING ORGANIZATION REPORT NUMBER

9. SPONSORING/MONITORING AGENCY NAME(S) AND ADDRESS(ES)
National Aeronautics and Space Administration
Washington, DC 20546-0001

10. SPONSOR/MONITOR'S ACRONYM(S)
NASA

11. SPONSOR/MONITOR'S REPORT NUMBER(S)
NASA/CR-2010-216699

12. DISTRIBUTION/AVAILABILITY STATEMENT
Unclassified - Unlimited
Subject Category 39
Availability: NASA CASI (443) 757-5802

13. SUPPLEMENTARY NOTES
Langley Technical Monitor: Dawn C. Jegley

14. ABSTRACT

A study was conducted to develop mass efficient composite struts. A closed-form design methodology for composite struts was developed using well established analyses to predict Euler buckling, local wall buckling, compression strength, damage tolerance, and interlaminar shear at geometric gradients. The methodology was coded in a spreadsheet suitable for convenient and rapid sizing of tapered composite struts. This spreadsheet analysis was used to determine the influence of several variables such as material stiffness, strut diameter, and material allowables on strut weight for given loading conditions. The comparison showed that, while the Park Aerospace design method was well suited to preliminary sizing for a conservative design, the closed-form-analyses-based spreadsheet accounts for all possible failure modes and is a good optimum strut design tool. The report concludes with a set of recommendations for future work in analytical design and analysis methodology enhancements.

15. SUBJECT TERMS
Composites; Structurally efficient; Graphite-epoxy; Tapered strut; Buckling

16. SECURITY CLASSIFICATION OF:			17. LIMITATION OF ABSTRACT	18. NUMBER OF PAGES	19a. NAME OF RESPONSIBLE PERSON
a. REPORT	b. ABSTRACT	c. THIS PAGE			STI Help Desk (email: help@sti.nasa.gov)
U	U	U	UU	43	19b. TELEPHONE NUMBER *(Include area code)* (443) 757-5802